Geochemistry of Eocene high-Mg# adakitic rocks in the northern Qiangtang terrane, central Tibet: Implications for early uplift of the plateau

JianLin Chen[1,†], JianBin Wu[1,2], JiFeng Xu[1,†], YanHui Dong[3], BaoDi Wang[4], and ZhiQiang Kang[5]

[1]*State Key Laboratory of Isotope Geochemistry, Guangzhou Institute of Geochemistry, Chinese Academy of Sciences, Guangzhou 510640, China*

[2]*University of Chinese Academy of Sciences, Beijing 100049, China*

[3]*Key Laboratory of Submarine Geosciences, Second Institute of Oceanography, State Oceanic Administration, Hangzhou 310012, China*

[4]*Chengdu Institute of Geology and Mineral Resources, Chengdu 610081, China*

[5]*Guilin University of Technology, Guilin 541004, China*

ABSTRACT

It is generally believed that the Tibetan Plateau is the result of crustal thickening in response to the collision of the Asian and Indian plates. However, the specific timing and uplift mechanism remain controversial. The widespread occurrence of Cenozoic lavas in the northern Qiangtang terrane provides a unique opportunity to constrain the dynamic processes that resulted in uplift of the northern Tibetan Plateau. Eocene lavas from the northern Qiangtang terrane display adakitic geochemical characteristics, such as high SiO_2 and Al_2O_3 contents, low Y and Yb contents, positive Sr anomalies, and high Sr/Y and La/Yb ratios, in combination with high Mg# (43–69) and negative anomalies for Nb and Ta, which suggest a garnet + rutile-in and plagioclase-free source residue. The same samples also have high K_2O and Th contents, high Th/Ce ratios, and low Nb/U, Ce/Pb, Ti/Eu, and Nd/Sm ratios, as well as high $^{87}Sr/^{86}Sr_{(i)}$ (0.7062–0.7075) and low $\varepsilon_{Nd(t)}$ (–6.3 to –2.9), which show a clear continental crust affinity. These high-Mg# adakitic rocks, combined with other characteristics of Tibetan Cenozoic lavas, indicate that they were derived from partial melting of delaminated lower continental crust, which subsequently reacted with surrounding mantle peridotites during ascent to crustal depths. The Eocene high-Mg# adakitic rocks (46–38 Ma), north-south–trending shoshonitic dikes (47–38 Ma), and contemporaneous mantle-derived Mg-rich potassic and shoshonitic lavas indicate that the thickness of the crust was at least 50 km before ca. 46 Ma, at which time rapid uplift and extension occurred, most likely caused by small-scale delamination of the lithospheric mantle at 46–38 Ma (Eocene) in central Tibet.

INTRODUCTION

Adakites were originally defined by Defant and Drummond (1990), following Kay (1978), as rocks resulting from partial melting of a subducted slab in the garnet stability field with special geochemical features, such as high Al_2O_3 and Sr, low Y and Yb contents, and high Sr/Y and La/Yb ratios. Subsequent studies on continental magmatism and experiment petrology (Rapp and Watson, 1995; Rapp et al., 1999) have revealed that similar geochemical signatures are also documented in Archean tonalite-trondhjemite-granodiorite (TTG) and igneous rocks from continental collisional orogens (Defant et al., 2002; Chung et al., 2003; Condie, 2005; Zhang et al., 2007; Q. Wang et al., 2008). It has already been accepted that adakitic rocks developed in continental collisional orogens provide significant geochemical constraints on the evolution of a thickened mafic lower continental crust (J.F. Xu et al., 2002a; Chung et al., 2003; Hou et al., 2004; Q. Wang et al., 2005, 2008). In some cases, high Mg# (molar Mg/[Mg + Fe]) adakitic rocks have been linked with lithospheric delamination, as exemplified by eastern China (J.F. Xu et al., 2002a; Gao et al., 2004; Q. Wang et al., 2006; Huang et al., 2008), Tibetan Plateau (Lai et al., 2003; Lai and Qin, 2008; Zhang et al., 2007; Liu et al., 2008; Q. Wang et al., 2008, 2010, Turkey (Karsli et al., 2010; Kadioglu and Dilek, 2010; Topuz et al., 2011; Shabanian et al., 2012), Iran (Shabanian et al., 2012), North America (Lee et al., 2006), and South America (Coldwell et al., 2011). In this sense, exploring the petrogenesis of adakitic rocks is the key to unraveling the continental crustal evolution in continental collisional orogens (Martin, 1999; Condie, 2005; Martin et al., 2005).

Details of the timing and mechanisms of uplift of the Tibetan Plateau have long been debated, such as whether the earliest uplift occurred at ca. 46 Ma in northern and northeastern Tibet (Chung et al., 1998, 2005; Guo et al., 2006; C. Wang et al., 2008; Q. Wang et al., 2008, 2010; Lai and Qin, 2013), or if the whole plateau was instead formed by one or more stages of uplift (Turner et al., 1993, 1996; Williams et al., 2001, 2004; Tapponnier et al., 2001; C. Wang et al., 2008; Chen et al., 2012). Changes in tectonic regime are typically marked by changes in the composition of associated magmatic products; as such, the extensive distribution of Cenozoic volcanic rocks throughout the Tibetan Plateau provides a good opportunity for understanding deep structural changes to the plateau during uplift, as well as changes at the surface (Turner et al., 1993; Chung et al., 2005). For example, based on the Cenozoic volcanic rocks from the plateau, Turner et al. (1993, 1996) argued that the convective thinning of underlying lithospheric mantle led to the uplift of the plateau at 13 Ma. In contrast, the differing ages of magmatic belts, coupled with other tectonic characteristics, led Tapponnier et al. (2001) to suggest that uplift of the plateau was stepwise, initiating in the central Tibet (Qiangtang terrane) during the Eocene before progressing northward and southward in response to the subduction of Asian or Indian continental lithosphere. Thus, the Cenozoic volcanism and uplift of the central plateau (Qiangtang terrane) have been explained by two distinct mechanisms: convective thinning (e.g., Turner et al., 1993, 1996; Chung et al., 1998; Miller et al., 1999; Williams et al., 2001) and intracontinental subduction (e.g., Roger et al., 2000; Tapponnier et al., 2001; Ding et al., 2003,

†E-mails: lzdxchen@gig.ac.cn; jifengxu@gig.ac.cn

GSA Bulletin; November/December 2013; v. 125; no. 11/12; p. 1800–1819; doi:10.1130/B30755.1; 13 figures; 2 tables.

2007; Guo et al., 2006; Q. Wang et al., 2008, 2010). Given this controversy, additional studies are required to decipher the petrogenesis of the Cenozoic volcanic rocks and corresponding uplift in the Qiangtang terrane of central Tibet.

In addition, it is believed that collisional orogenic belts should have a thickened crust and associated lithospheric keel. However, a principal result of deep seismic profiling worldwide has been the recognition that old collisional orogens in fact lack substantial crustal roots or lithospheric keels (e.g., Nelson, 1992; Gao et al., 1998; Lustrino, 2005; Kenzie and Priestley, 2008), which is believed to be the consequence of delamination (e.g., Bird, 1979; Nelson, 1992). This contrasts markedly to active collision zones such as the Alps and the Himalayan–Tibetan Plateau, which exhibit substantially thickened and inhomogeneous crust, and even subcontinental lithospheric mantle (e.g., Nelson, 1992; Gao et al., 1998; Kenzie and Priestley, 2008). The role of delamination in the uplift of the Tibetan Plateau is also still debated (e.g., Wu et al., 2008). Thus, further work is required to prove whether delamination of thickened lower crust and/or subcontinental lithospheric mantle is an important process within collisional orogens (e.g., Bird, 1979; Nelson, 1992; Gao et al., 1998).

In this paper, we report new geochemical data for the Luanqinshan, Yuejinla, Dongyuehu, and Meiriqiecuo Eocene lavas from the northern Qiangtang terrane. Combined with previous geochemical data for coeval rocks in the Qiangtang terrane (such as the Eocene adakitic rocks, Mg-rich potassic rocks, and shoshonitic rocks), these data allow us to infer the composition of their source materials, and corresponding formation mechanisms. The new geochemical data indicate that they have the characteristics of high-Mg# adakitic rocks, which were probably derived from melting of delaminated lower crust. Their distinctive petrogenesis, combined with evidence from mantle-derived Mg-rich potassic rocks and shoshonitic rocks from the Qiangtang terrane, provides an important constraint on the timing and mechanisms of early uplift in central Tibet.

BACKGROUND

On a regional scale, the Tibetan Plateau is composed of a tectonic collage of continental terranes (blocks). From north to south, the plateau is predominantly made up of the following E-W–trending terranes (Fig. 1A): the Songpan-Ganzi, Qiangtang, Lhasa, and Himalayan (Yin and Harrison, 2000). These terranes are separated by the Jinsha, Bangong, and Indus-Yalu sutures, which represent fragments of the Paleotethys, Midtethys, and Neotethys Oceans, respectively (Yin and Harrison, 2000).

A Late Triassic to Early Jurassic east-west–trending belt of blueschist-bearing mélange is present in the center of the Qiangtang terrane (Kapp et al., 2000, 2003) and has been interpreted as representing a distinct suture zone separating a northern Qiangtang terrane of Cathaysian affinity from a southern Qiangtang terrane of Gondwanan affinity (Li et al., 1995). The Qiangtang terrane contains many Cretaceous marine limestones (Deng, 1998), as well as widespread E-W–trending Paleogene nonmarine basins, filled with fluvial sandstone and conglomerate, and lacustrine limestone and mudstone (Ding et al., 2003).

Cenozoic magmatic volcanic and subordinate intrusive rocks are unevenly distributed throughout the Qiangtang terrane and are mainly concentrated in the northern part of the Terrane (Fig. 1A), including high-Mg potassic rocks, shoshonitic rocks, and calc-alkaline lavas, predominantly with eruption ages of 50–28 Ma (e.g., Zheng et al., 1996; Chi et al., 1999; Deng, 1998; Tan et al., 2000; Roger et al., 2000; Yin and Harrison, 2000; J.H. Wang et al., 2001; Lin, 2003; Lin et al., 2003; Ding et al., 2003, 2007; Williams et al., 2004; Wei et al., 2004; Li et al., 2005; Spurlin et al., 2005; Jiang et al., 2006; Guo et al., 2006; Liang et al., 2007; C. Wang et al., 2008; Q. Wang et al., 2008, 2010; B.D. Wang et al., 2010; Dong et al., 2008; S. Liu et al., 2008; J.F. Liu et al., 2009; Lai and Qin, 2013), in addition to a minority with ages of 5–0 Ma (e.g., Deng, 1998; Hacker et al., 2000). The lavas of the Duogecuoren-Wuerkengwula mountains area in the northern Qiangtang terrane display the largest outcrop areas of all Cenozoic magmatic rocks in the central-northern Tibetan Plateau (Figs. 1A and 1B). The Eocene volcanic rocks are widely distributed in the Duogecuoren area in outcrops that range from 600–700 m^2 to several square kilometers in size (Q. Wang et al., 2008) (Fig. 1B). Eocene volcanic rocks in Wuerkengwula mountains area cover an area of 2500 km^2 (Lin, 2003; Lin et al., 2003), which occur as lava sheets that range in thickness from 10 to 425 m. They unconformably overlie the Jurassic and Cretaceous sedimentary rocks (Lin, 2003; Lin et al., 2003; Lai and Qin, 2013). The Luanqinshan, Yuejinla, Dongyuehu, and Meiriqiecuo lavas erupted at 39.8–43.7 Ma (Q. Wang et al., 2008), 39.9–43.7 Ma (Q. Wang et al., 2008), 44.5 Ma (Dong et al., 2008; Q. Wang et al., 2008), and 43.4 Ma (this study), respectively (Fig. 1B).

The Luanqinshan, Yuejinla, Dongyuehu, and Meiriqiecuo volcanic rocks include light-gray and gray trachyandesites, trachytes, andesites, and dacites, all in massive structure and typical porphyritic textures. The trachyandesites and trachytes exhibit a trachytic groundmass texture and contain more phenocrysts (5%–20%) than the andesites and dacites (<5%). The main phenocryst phases in trachyandesites and trachytes are plagioclase and pyroxene, with less sanidine, biotite, amphibole, and quartz, and minor Fe-Ti oxides, apatite, and zircon. Some biotite and amphibole crystals exhibit dark margins, while quartz has embayed textures. Andesites and dacites have the same mineralogy as trachyandesites and trachytes.

ANALYTICAL TECHNIQUES

Selected fresh pieces of whole rock were sawn into chips and were ultrasonically cleaned, first in distilled water with <5% HNO_3, and then in distilled water alone; they were subsequently dried, and visible contamination was removed by handpicking. The rocks were then crushed and subsequently ground in an agate ring mill, and the resulting powder was analyzed for major and trace elements, as well as Sr and Nd isotopes, at the Guangzhou Institute of Geochemistry, Chinese Academy of Sciences (GIGCAS), Guangzhou, China.

Bulk-rock major-element abundances were determined using an X-ray fluorescence spectrometer (XRF), following analytical procedures described by Goto and Tatsumi (1996). The analytical uncertainties for the major elements analyzed were generally better than 5% (Chen et al., 2010). Bulk-rock trace-element data were obtained by inductively coupled plasma–mass spectrometry (ICP-MS) following the analytical procedure described by Chen et al. (2010). The precision of rare earth element (REE) and high field strength element (HFSE) concentrations obtained using this method is estimated to be 5% (Chen et al., 2010). Sr and Nd isotopic compositions were measured using a Micromass Isoprobe multicollector–inductively coupled plasma–mass spectrometer (MC-ICP-MS) at GIGCAS, using analytical procedures that have been described by X.H. Li et al. (2004), Wei et al. (2002), and Chen et al. (2010). Chemical separation of Sr and Nd from matrix was performed using methods similar to those described by Li and McCulloch (1998), J.F. Xu et al. (2002b), and Chen et al. (2010). Measured $^{87}Sr/^{86}Sr$ values of the NBS987 standard and $^{143}Nd/^{144}Nd$ values of the JNdi-1 standard were 0.710288 ± 0.000028 ($2\sigma_m$) and 0.512109 ± 0.000012 ($2\sigma_m$), respectively; all measured $^{143}Nd/^{144}Nd$ and $^{87}Sr/^{86}Sr$ values were fractionation corrected to $^{146}Nd/^{144}Nd = 0.7219$ and $^{86}Sr/^{88}Sr = 0.1194$, respectively.

The $^{40}Ar/^{39}Ar$ dating was performed using a GV5400 Ar-Ar mass spectrometer; details of

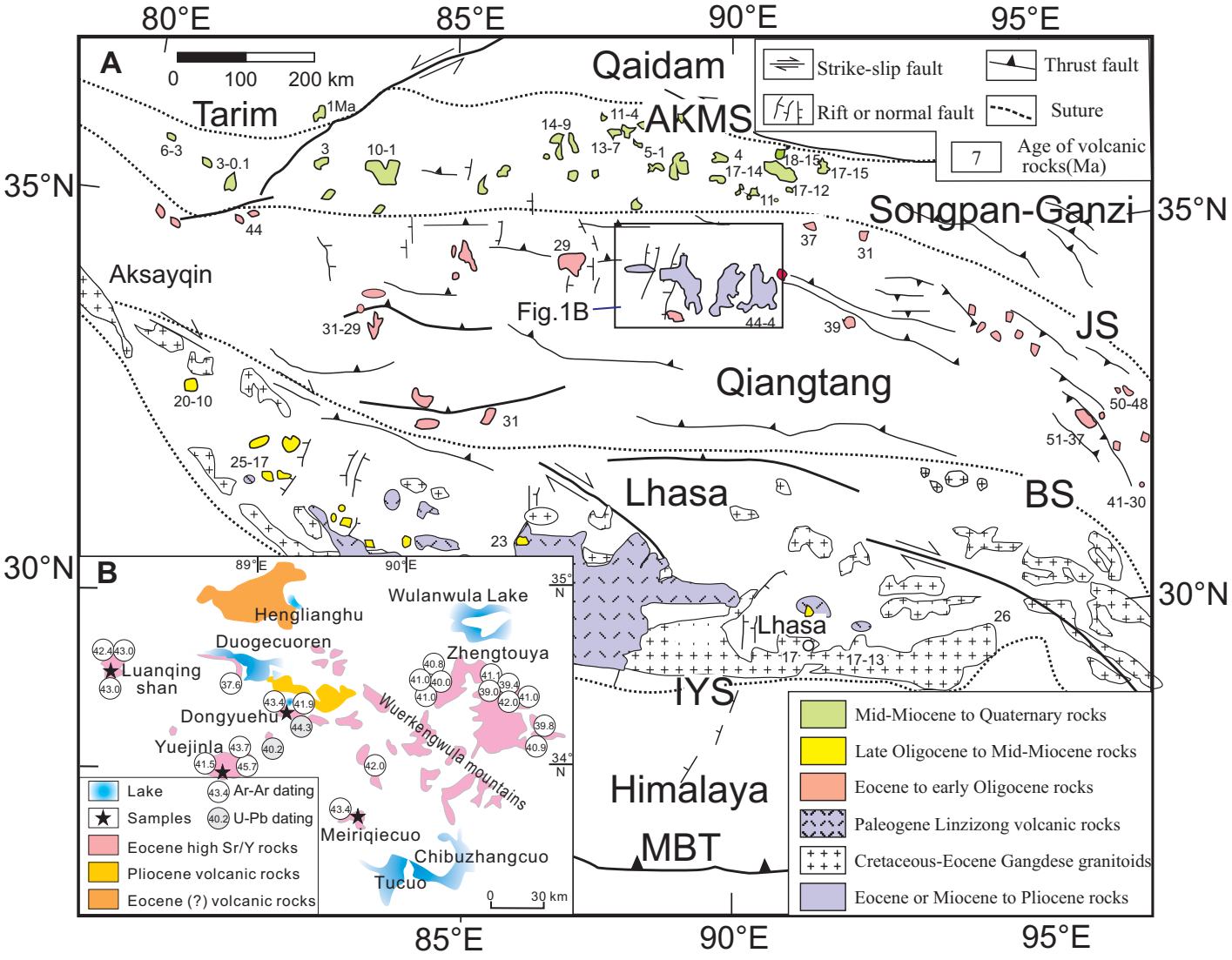

Figure 1. (A) Map of the Tibetan Plateau showing major crustal terranes, as well as the temporal and spatial distribution of Cenozoic volcanic rocks (modified from Yin and Harrison, 2000; Chung et al., 2005; Q. Wang et al., 2008). Age data for volcanic rocks are from previous studies (Turner et al., 1996; Chung et al., 1998; J.H. Wang et al., 2001; Ding et al., 2003; Hou et al., 2004; Lai et al., 2003; Chung et al., 2005; Spurlin et al., 2005; Q. Wang et al., 2005; Jiang et al., 2006; Ding et al., 2007; Liang et al., 2007; Mo et al., 2007; C. Wang et al., 2008; Dong et al., 2008). The main suture zones between major terranes are also shown, where AKMS—Anyimaqen–Kunlun–Muztagh suture, JS—Jinshajiang suture, BS—Bangong suture, and IYS—Indus-Yalu suture. MBT—Main Boundary thrust. (B) Simplified geological map showing outcrops of magmatic rocks in the Duogecuoren area, northern Qiangtang terrane, Tibetan Plateau (modified from Dong, 2008). Age data for volcanic rocks are from Lin (2003), Lin et al. (2003), Q. Wang et al. (2008, 2010), and this study.

the experimental procedures can be found in Qiu and Jiang (2007). Argon gas was extracted from the sample by step-heating using a MIR10 CO_2 continuous wave laser. The released gases were purified by two Zr/Al getter pumps operated for 5–8 min at room temperature and ~450 °C, respectively. The background level of the sample holder was lower than 2 mV prior to analysis, while the signal of the sample was generally between 40 and 200 mV. The $^{40}Ar/^{39}Ar$ dating results were calculated and plotted using the ArArCALC software by Koppers (2002). Using the ZBH-2506 biotite (132 Ma) as a flux monitor, the J-value was determined to be 0.00955.

CHRONOLOGY AND GEOCHEMISTRY

Chronology

Prior to the present study, only three K-Ar ages (36.3 ± 0.9 Ma, 36.8 ± 1.0 Ma, and 38.9 ± 1.0 Ma) had been reported for the Meiriqiecuo lava (Lin, 2003). In the present study, analysis of a Meiriqiecuo lava (sample D6441) yielded a $^{40}Ar/^{39}Ar$ plateau age of 43.35 ± 0.22 Ma (Fig. 2; Table 1). Thus, we considered that the Meiriqiecuo lava was mainly erupted at 43.35 ± 0.22 Ma. These results, together with previously published high-quality ages (e.g., $^{40}Ar/^{39}Ar$ or zircon U-Pb ages; e.g., Chi et al., 1999; Lin, 2003; Lin et al., 2003; B.H. Li et al., 2004; Zhao et al., 2007; C. Wang et al., 2008; Q. Wang et al., 2008, 2010), indicate that the largest lavas

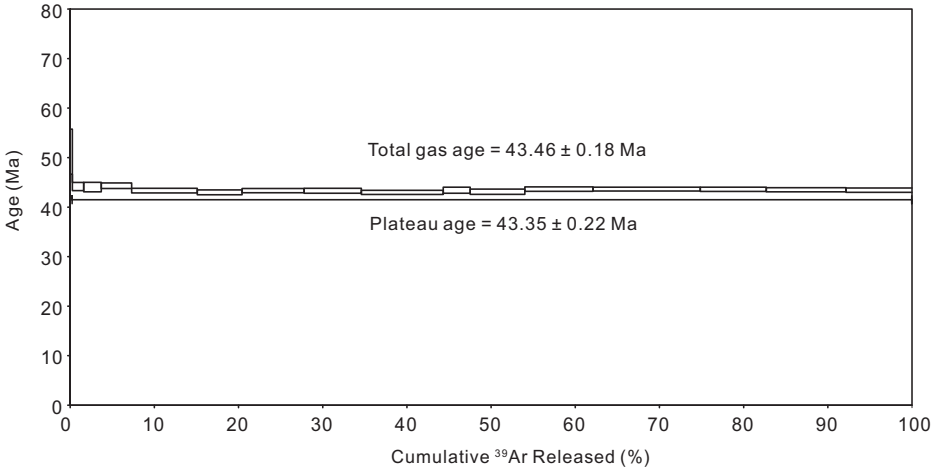

Figure 2. $^{40}Ar/^{39}Ar$ age spectra for a bulk-rock sample of an adakitic rock from the Meiriqiecuo area in the northern Qiangtang terrane (uncertainties are displayed as 2σ).

of the Duogecuoren–Wuerkengwula mountains area that outcrop in the central-northern Tibetan Plateau were mainly erupted from 46 to 38 Ma (Q. Wang et al., 2008) (Fig. 3).

Major- and Trace-Element Geochemistry

In Figure 4A, we present a plot of (Na_2O + K_2O) versus SiO_2 for the volcanic rocks of Luanqinshan, Yuejinla, Dongyuehu, and Meiriqiecuo, which include trachyandesites, trachytes, andesites, and dacites (see also Table 2). On a K_2O versus SiO_2 plot (Fig. 4B), most samples are potassium-rich ($K_2O/Na_2O > 0.5$).

In major-element Harker diagrams (Fig. 5), the contents of TiO_2, MgO, and CaO decrease with increasing SiO_2, whereas Na_2O, Al_2O_3, and P_2O_5 show no obvious correlation. The samples have lower MgO, CaO, TiO_2, Na_2O, P_2O_5, and K_2O, similar Na_2O, and higher Al_2O_3 contents than ultrapotassic (Holbig and Grove, 2008) and Mg-rich potassic rocks (MgO ≥ 6%, K_2O/Na_2O ≥ 1) from the northern Qiangtang terrane (Williams et al., 2004; Guo et al., 2006; Zhao et al., 2009a; Chen et al., 2012) (Figs. 4 and 5). These geochemical differences probably reflect the contrasting compositions of the source in each case. However, they have similar MgO, CaO, Al_2O_3, TiO_2, Na_2O, P_2O_5, and K_2O contents to the adakitic rocks in eastern China that were derived by partial melting of the delaminated lower crust (e.g., J.F. Xu et al., 2002a; Gao et al., 2004; W.L. Xu et al., 2006).

Plots of SiO_2 versus trace-element concentrations (Fig. 6) for samples of this study from the northern Qiangtang terrane indicate that concentrations of Sr, Cr, and Ni decrease with increasing SiO_2, whereas Ba shows no correlation. When compared with mafic granulite xenoliths from the northern Qiangtang terrane (Lai and Qin, 2008), the samples in this study have distinctly higher Sr, Ba, Cr, and Ni concentrations. In addition, they have similar Cr and Ni concentrations to the adakitic rocks in eastern China that were derived by partial melting of the delaminated lower crust (e.g., J.F. Xu et al., 2002a; Gao et al., 2004; W.L. Xu et al., 2006).

Chondrite-normalized REE patterns of the samples in this study (Figs. 7A–7D) have light REE (LREE)–enriched and heavy REE (HREE)–depleted patterns ($[La/Yb]_N$ = 13.3–54.9), with a lack of obvious negative Eu anomalies. The depleted and flat HREE patterns probably resulted from the presence of residual garnet and amphibole in their source, according to high-pressure–high-temperature (*P-T*) melting experiments with mafic rocks (Xiong, 2006). In addition, their REE concentrations and patterns are similar to those in the adakitic rocks derived by partial melting of the delaminated garnet-bearing lower crust in eastern China (e.g., J.F. Xu et al., 2002a; Gao et al., 2004; W.L. Xu et al., 2006). Moreover, the samples in this study also have Gd/Yb values (>2) that are similar to those in the adakitic rocks from the eclogite-facies basaltic slab in the central Trans-Mexican volcanic belt (Mori et al., 2007).

On primitive mantle–normalized spider diagrams (Figs. 7E–7H), the samples of this study are characterized by enrichments in large ion lithophile elements (LILEs) such as Rb, Ba, Th, and U. They also exhibit enrichments in the LREE, pronounced negative anomalies for HFSE such as Nb, Ta, and Ti, and distinct positive Sr anomalies. The samples in this study also have similar patterns to the adakitic rocks produced by partial melting of the delaminated

TABLE 1. RESULTS OF ARGON ISOTOPE ANALYSES OF ADAKITIC ROCKS FROM THE MEIRIQUECUO AREA IN THE NORTHERN QIANGTANG TERRANE

Incremental heating		^{36}Ar (a)	^{37}Ar (ca)	^{38}Ar (cl)	^{39}Ar (k)	^{40}Ar (r)	^{40}Ar(r) (%)	^{39}Ar(k) (%)	Age ± 2σ (Ma)
Sample D6441 (whole rocks), T1 = 43.45 ± 0.22 Ma, T2 = 43.46 ± 0.18 Ma, T3 = 43.32 ± 0.41 Ma, T4 = 43.13 ± 0.39 Ma, MSWD = 1.96.									
06M2060B	3.00 W	0.00000	0.00084	0.00000	0.00055	0.00133	56.20	0.26	51.20 ± 4.54
06M2060C	3.00 W	0.00000	0.00562	0.00000	0.00283	0.00584	82.67	1.34	44.16 ± 0.83
06M2060D	5.00 W	0.00000	0.01136	0.00000	0.00440	0.00906	86.66	2.09	44.04 ± 0.96
06M2060E	6.00 W	0.00001	0.02304	0.00000	0.00761	0.01577	87.33	3.61	44.32 ± 0.57
06M2060G	6.80 W	0.00001	0.05059	0.00000	0.01646	0.03332	92.67	7.80	43.33 ± 0.47
06M2060H	7.30 W	0.00001	0.03241	0.00000	0.01122	0.02253	93.54	5.32	42.98 ± 0.49
06M2060I	8.00 W	0.00001	0.04570	0.00000	0.01557	0.03154	92.78	7.38	43.34 ± 0.43
06M2060J	8.70 W	0.00001	0.04076	0.00000	0.01432	0.02898	92.72	6.79	43.29 ± 0.50
06M2060L	9.50 W	0.00001	0.06251	0.00000	0.02054	0.04124	93.77	9.73	42.98 ± 0.42
06M2060M	10.30 W	0.00001	0.01861	0.00000	0.00675	0.01369	88.12	3.20	43.41 ± 0.60
06M2060N	11.00 W	0.00001	0.04174	0.00001	0.01370	0.02760	88.92	6.49	43.12 ± 0.53
06M2060O	12.00 W	0.00001	0.05550	0.00000	0.01709	0.03485	94.68	8.10	43.63 ± 0.45
06M2060Q	13.50 W	0.00001	0.08110	0.00001	0.02688	0.05481	93.72	12.74	43.64 ± 0.39
06M2060R	15.00 W	0.00000	0.05222	0.00000	0.01656	0.03374	95.77	7.85	43.59 ± 0.43
06M2060S	17.00 W	0.00000	0.05983	0.00001	0.01997	0.04060	96.51	9.46	43.51 ± 0.42
06M2060T	20.00 W	0.00000	0.05106	0.00000	0.01656	0.03360	96.41	7.85	43.43 ± 0.44

Note: T1—plateau age; T2—molten age; T3—normal isochron; T4—inverse isochron; MSWD—mean square of weighted deviates.

^{36}Ar(a) is from the atmosphere; ^{37}Ar (ca) is produced from ^{40}Ca; ^{38}Ar (cl) is derived from ^{38}Cl; ^{39}Ar (k) is produced from ^{39}K during the irradiation; ^{40}Ar (r) is the radiogenic argon from ^{40}K.

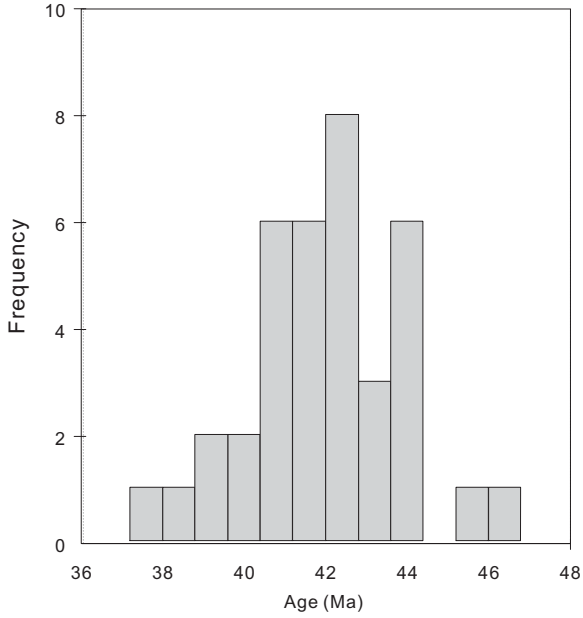

Figure 3. Age distribution of Eocene lavas from the northern Qiangtang terrane (data are from Chi et al., 1999; Lin, 2003; Lin et al., 2003; B.H. Li et al., 2004; Q. Wang et al., 2008, 2010; this study).

lower crust in eastern China (e.g., J.F. Xu et al., 2002a; Gao et al., 2004; W.L. Xu et al., 2006).

Major- and trace-element results indicate that our samples from the northern Qiangtang terrane show adakitic compositional characteristics: They are characterized by high SiO_2 (≥56 wt%), Al_2O_3 (14.5–16.7 wt%), and Sr (816–2276 ppm), and low HREE contents (e.g., Y = 6.6–16.9 ppm and Yb = 0.63–1.45 ppm), and they have high $(La/Yb)_N$ (13.3–54.9), Sr/Y (78–269), and Gd/Yb (>2) ratios, similar to adakites from subduction-zone settings (Sr > 400 ppm, Y < 18 ppm, Yb < 1.9 ppm) (Figs. 8A, 8B, 8C; Defant and Drummond, 1990; Mori et al., 2007; Castillo, 2012) that show a garnet signature in their source. In addition, they also have geochemical characteristics similar to the adakitic rocks produced by the partial melting of the eclogite-facies basaltic slab in the central Trans-Mexican volcanic belt (Mori et al., 2007) and the adakitic melts produced by partial melting of the delaminated garnet-bearing lower continental crust in eastern China (e.g., J.F. Xu et al., 2002a; Gao et al., 2004; W.L. Xu et al., 2006). Moreover, they have relatively high MgO contents (1.7–6.0 wt%), high Mg# (Mg# = $100 \times Mg^{2+}/[Fe^{2+} + Mg^{2+}]$, 43–69), and high Cr and Ni concentrations (Table 2; Figs. 5, 6, and 8D). We therefore choose to refer to our samples as "high-Mg# adakitic rocks."

The high Sr/Y and Gd/Yb ratios, low HREE concentrations, negative anomalies for Nb and Ta, lack of obvious negative Eu anomalies, and positive Sr anomalies in the rocks of this study imply partial melting in the presence of residual garnet + rutile and amphibole, but not plagioclase (Martin, 1987; Xiong et al., 2006). In addition, their distinctly high Zr/Hf ratios (37–48) indicate the existence of clinopyroxene and amphibole in the residue (David et al., 2000; Linnen and Keppler, 2002; Pfänder et al., 2007).

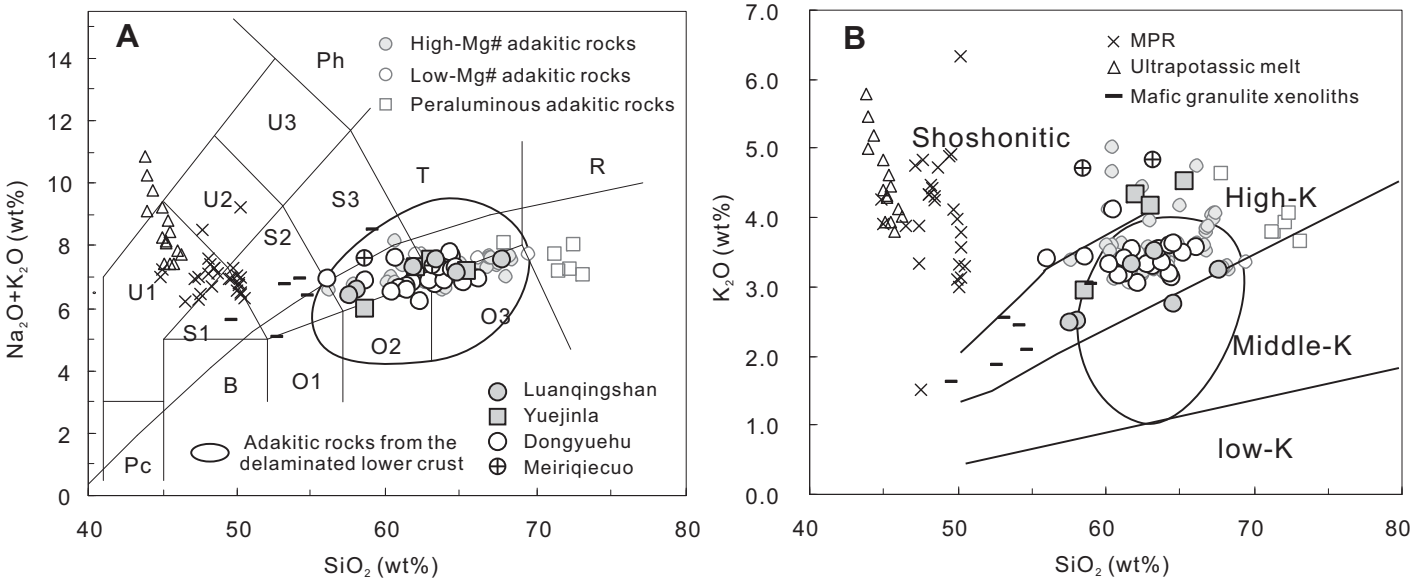

Figure 4. (A) ($Na_2O + K_2O$) vs. SiO_2 diagram (total alkali–silica [TAS]) (from Le Bas et al., 1986) showing data for Eocene high-Mg# adakitic rocks, and Mg-rich potassic rocks (MPR) from the Qiangtang terrane (Williams et al., 2004; Guo et al., 2006; Zhao et al., 2009a; Chen et al., 2012); ultrapotassic melts (Holbig and Grove, 2008); mafic granulite xenoliths from the northern Qiangtang terrane (Lai and Qin, 2008); adakitic rocks from delaminated lower crust (J.F. Xu et al., 2002a; Gao et al., 2004; W.L. Xu et al., 2006); high-Mg# adakitic rocks (Q. Wang et al., 2008; Lai and Qin, 2013), low-Mg# adakitic rocks (Lai and Qin, 2013), and peraluminous adakitic rocks (Q. Wang et al., 2008) from northern Qiangtang terrane. The following abbreviations are used: B—basalt, O1—basaltic andesite, O2—andesite, O3—dacite, R—rhyolite, S1—trachybasalt, S2—basaltic trachyandesite, S3—trachyandesite, T—trachyte, U1—tephrite/basanite, U2—phonotephrite, U3—tephriphonolite, Pc—picrobasalt, and Ph—phonolite. (B) SiO_2 vs. K_2O diagram for Cenozoic volcanic rocks from central Tibet; all other data sources and symbols are the same as part A.

TABLE 2. MAJOR- (WT%) AND TRACE-ELEMENT (PPM) CONCENTRATIONS, AS WELL AS Sr AND Nd ISOTOPE COMPOSITIONS, FOR HIGH-Mg# ADAKITIC ROCKS FROM THE NORTHERN QIANGTANG TERRANE

Sample	04LQS-2	04LQS-3	04LQS-6	04LQS-14	04LQS-16	04YJL-05	04JYL-07	04YJL-06
Location			Luanqingshan				Yuejinla	
SiO_2	61.64	63.15	57.77	67.38	64.40	58.44	61.20	62.99
TiO_2	0.50	0.55	0.77	0.44	0.55	0.79	0.83	0.83
Al_2O_3	14.84	15.00	15.41	15.88	16.26	15.19	15.20	15.89
Fe_2O_3	4.80	4.83	6.16	3.33	4.56	7.18	5.26	4.71
MnO	0.07	0.04	0.09	0.05	0.05	0.09	0.07	0.06
MgO	5.43	4.01	4.65	1.66	2.26	5.73	4.37	3.56
CaO	5.20	4.68	7.71	3.17	4.56	6.34	4.48	4.31
Na_2O	3.95	3.95	4.01	4.24	4.29	3.03	2.94	3.34
K_2O	3.31	3.52	2.49	3.23	2.75	2.93	4.28	4.17
P_2O_5	0.06	0.06	0.47	0.15	0.03	0.04	0.08	0.09
LOI	0.86	1.73	2.28	0.25	1.05	0.63	0.67	0.55
Total	100.67	101.50	101.81	99.79	100.74	100.39	99.36	100.49
Mg#	69.35	62.42	60.15	49.96	49.84	61.49	62.44	60.20
Sc	10.93	10.28	12.90	5.51	10.53	16.65	8.51	6.92
Cr	212	253	209	33.65	88.43	368	176	159
Co	17.20	13.01	21.08	7.22	11.11	24.71	17.91	16.05
Ni	146	125	150	23.89	64.45	173	92.20	82.01
Rb	84.24	95.07	55.96	98.82	72.56	84.64	157	158
Ba	1741	1880	1520	1296	1456	1957	1923	2255
Th	16.95	15.79	14.88	19.65	8.73	13.44	29.08	23.61
U	3.15	2.63	3.49	4.13	2.70	3.80	8.74	7.42
Nb	7.56	8.31	11.87	4.90	5.53	9.61	14.52	13.62
Ta	0.47	0.50	0.69	0.33	0.43	0.66	1.14	0.96
La	56.13	47.74	73.12	52.24	18.23	44.95	69.80	60.24
Ce	92.16	70.00	128	90.00	30.29	92.90	118	103
Pb	36.58	40.37	27.97	30.03	25.48	62.56	40.21	37.76
Pr	10.27	7.59	14.46	10.12	3.43	7.98	12.89	11.18
Sr	2276	2113	2118	816	1248	1876	1552	1747
Nd	36.61	26.41	51.17	34.72	13.00	28.65	43.63	38.37
Zr	183	199	217	239	157	211	299	306
Hf	4.45	4.79	4.68	5.80	4.20	5.11	6.71	7.09
Sm	5.39	3.93	7.34	5.07	2.45	4.66	6.13	5.22
Eu	1.45	1.70	1.79	1.08	0.88	1.21	1.60	1.66
Gd	2.77	2.13	4.34	2.86	1.79	3.10	3.44	2.84
Tb	0.41	0.34	0.66	0.41	0.29	0.45	0.49	0.43
Dy	1.82	1.65	3.27	1.80	1.62	2.45	2.42	2.00
Y	8.99	7.85	16.60	8.49	7.77	11.96	11.74	9.58
Ho	0.32	0.29	0.59	0.33	0.31	0.49	0.43	0.35
Er	0.84	0.75	1.45	0.81	0.84	1.24	1.14	0.93
Tm	0.13	0.12	0.21	0.12	0.14	0.19	0.15	0.12
Yb	0.89	0.83	1.45	0.79	0.98	1.21	0.96	0.79
Lu	0.14	0.14	0.24	0.13	0.17	0.19	0.15	0.13
Th/U	5.38	6.00	4.27	4.76	3.23	3.54	3.33	3.18
Th/Ce	0.18	0.23	0.12	0.22	0.29	0.14	0.25	0.23
$^{87}Sr/^{86}Sr$	0.706538	0.706662	0.706750	0.707200	0.706421	0.706269	0.707048	0.707061
$^{87}Sr/^{86}Sr_{(i)}$	0.706477	0.706589	0.706707	0.707001	0.706325	0.706194	0.706882	0.706913
$^{143}Nd/^{144}Nd$	0.512461	0.512454	0.51244	0.512445	0.512459	0.512370	0.512382	0.51236
$\varepsilon_{Nd(t)}$	–2.9	–3.1	–3.3	–3.2	–3.1	–4.7	–4.4	–4.8
T_{DM} (Ga)	0.85	0.86	0.83	0.86	1.06	1.03	0.91	0.92
Sample	04YJL-09	04DN30-2	04DN30-3	04DN31-1	04DN32-1	04DN32-2	04DN35-2	04DN36-3
Location	Yuejinla				Dongyuehu			
SiO_2	64.22	55.47	61.07	62.17	64.17	63.91	62.83	60.93
TiO_2	0.70	1.02	0.74	0.83	0.69	0.69	0.79	0.92
Al_2O_3	14.51	15.27	15.53	16.06	16.03	16.15	15.96	15.90
Fe_2O_3	4.40	7.09	5.55	5.20	4.73	4.95	5.24	5.70
MnO	0.06	0.10	0.08	0.08	0.03	0.03	0.05	0.09
MgO	3.66	6.01	4.49	3.36	1.99	1.83	2.57	4.10
CaO	3.63	6.87	4.66	4.43	4.36	4.13	4.11	5.00
Na_2O	2.62	3.48	3.23	3.50	4.49	4.54	3.46	3.17
K_2O	4.45	3.37	3.51	3.29	3.12	3.17	3.30	3.38
P_2O_5	0.09	0.25	0.08	0.05	0.04	0.04	0.14	0.21
LOI	1.72	1.20	1.00	0.62	0.85	0.93	1.64	1.19
Total	100.04	100.13	99.94	99.61	100.48	100.37	100.10	100.57
Mg#	62.47	62.92	61.81	56.40	45.66	42.57	49.58	58.99
Sc	8.34	17.77	10.59	9.40	10.17	10.07	10.57	11.26
Cr	151	362	206	116	121	127	132	162
Co	14.64	29.75	18.77	16.50	11.53	10.39	12.41	20.76
Ni	73.63	144	101	67.31	59.25	56.58	72.70	85.75
Rb	181	86.55	118	100	98.51	103	107	113
Ba	1844	1786	1838	1757	1968	2064	1356	1290
Th	22.74	22.38	22.99	19.08	13.06	13.31	16.11	15.79
U	6.33	4.91	4.96	4.38	3.13	2.76	4.07	4.25
Nb	12.73	14.76	9.81	10.60	7.78	7.47	9.33	9.17
Ta	0.98	0.85	0.59	0.65	0.50	0.51	0.60	0.65
La	61.89	61.76	52.40	43.85	25.13	27.32	26.72	43.22
Ce	110	112	88.65	69.74	45.76	43.89	46.57	73.92

(*continued*)

TABLE 2. MAJOR- (WT%) AND TRACE-ELEMENT (PPM) CONCENTRATIONS, AS WELL AS Sr AND Nd ISOTOPE COMPOSITIONS, FOR HIGH-Mg# ADAKITIC ROCKS FROM THE NORTHERN QIANGTANG TERRANE (*continued*)

Sample	04YJL-09	04DN30-2	04DN30-3	04DN31-1	04DN32-1	04DN32-2	04DN35-2	04DN36-3
Location	Yuejinla				Dongyuehu			
Pb	38.34	17.48	32.45	26.02	6.98	5.15	23.40	31.52
Pr	12.25	13.00	9.37	7.25	4.75	5.16	5.02	8.38
Sr	1095	1669	1135	1073	959	1030	892	917
Nd	41.37	47.30	31.11	24.29	17.19	19.18	17.83	30.15
Zr	282	305	263	273	206	198	221	228
Hf	6.54	6.87	5.93	5.86	5.09	4.85	5.39	5.41
Sm	5.93	7.11	4.40	3.46	3.01	3.15	2.78	4.82
Eu	1.43	2.16	1.38	1.38	1.02	1.15	1.16	1.41
Gd	3.38	4.16	2.50	2.06	2.04	2.19	1.76	3.16
Tb	0.54	0.62	0.39	0.32	0.32	0.32	0.27	0.47
Dy	2.68	3.16	1.99	1.66	1.74	1.72	1.47	2.44
Y	13.23	15.40	9.89	8.07	8.47	8.36	6.63	11.75
Ho	0.50	0.60	0.37	0.31	0.34	0.34	0.28	0.44
Er	1.32	1.51	0.99	0.80	0.88	0.87	0.70	1.13
Tm	0.19	0.21	0.14	0.12	0.13	0.13	0.10	0.16
Yb	1.17	1.33	0.91	0.73	0.81	0.81	0.63	1.01
Lu	0.19	0.20	0.15	0.12	0.13	0.13	0.10	0.16
Th/U	3.59	4.55	4.64	4.36	4.17	4.83	3.96	3.71
Th/Ce	0.21	0.2	0.26	0.27	0.29	0.3	0.35	0.21
$^{87}Sr/^{86}Sr$	0.707746	0.706884		0.707270			0.707023	0.707697
$^{87}Sr/^{86}Sr_{(t)}$	0.706913	0.706715		0.707105			0.706847	0.707479
$^{143}Nd/^{144}Nd$	0.512287	0.512436		0.512386			0.512434	0.512369
$\varepsilon_{Nd(t)}$	–6.2	–3.3		–4.3			–3.4	–4.7
T_{DM} (Ga)	1.04	0.89		0.82			0.92	1.02

Sample	04DN37-2	04DN39	04DN40	04DY44-2	04DY44-4	04DY44-7	04D6441	04D6437
Location			Dongyuehu				Meiriqiecuo	
SiO_2	57.91	62.90	65.55	59.41	63.77	60.04	63.15	58.53
TiO_2	0.90	0.84	0.55	0.88	0.60	0.82	0.77	0.96
Al_2O_3	16.65	15.89	15.27	16.11	15.32	15.79	14.12	15.19
Fe_2O_3	5.72	5.67	3.86	5.84	4.44	5.48	5.74	6.09
MnO	0.12	0.09	0.04	0.07	0.17	0.05	0.09	0.06
MgO	4.24	2.78	2.85	3.83	3.36	3.67	4.35	4.04
CaO	6.40	4.51	4.04	5.81	4.21	5.74	4.17	5.30
Na_2O	3.43	3.44	3.33	3.11	3.58	3.43	2.48	2.90
K_2O	3.39	3.29	3.55	3.29	3.56	4.08	4.85	4.71
P_2O_5	0.06	0.14	0.05	0.19	0.13	0.02	0.03	0.08
LOI	1.21	0.84	1.34	1.57	0.82	0.76	0.12	1.51
Total	100.03	100.41	100.41	100.10	99.97	99.88	99.86	99.37
Mg#	59.73	49.54	59.63	56.76	60.19	57.23	60.28	56.99
Sc	16.81	9.13	7.02	13.82	8.54	10.84	13.62	14.67
Cr	307	235	169	291	183	206	158	188
Co	20.81	10.99	16.50	17.31	23.39	17.08	17.23	19.03
Ni	97.52	86.18	103	104	132	88.09	58.87	111
Rb	86.32	127	117	109	127	105	154	108
Ba	1447	1300	1483	1358	1952	2120	2757	3648
Th	11.16	17.71	17.50	16.08	19.19	13.44	20.45	23.02
U	3.89	5.02	4.59	4.46	5.07	3.82	4.64	5.58
Nb	9.11	7.07	8.48	9.53	7.57	8.90	14.00	16.29
Ta	0.65	0.52	0.57	0.67	0.50	0.53	0.93	0.94
La	18.06	33.71	50.14	41.63	50.61	49.22	49.42	66.50
Ce	32.90	58.02	92.73	75.59	91.11	81.60	85.78	106
Pb	33.10	19.46	35.43	40.78	30.26	13.69	24.02	40.49
Pr	3.83	6.10	10.37	8.94	9.70	8.30	8.34	11.24
Sr	1281	851	1220	1152	1519	1907	1770	2827
Nd	15.09	20.81	35.14	31.83	33.15	28.30	27.66	39.29
Zr	231	180	217	217	212	207	185	302
Hf	5.51	4.46	5.27	5.08	5.10	4.91	4.49	6.31
Sm	2.80	3.18	5.13	4.84	4.77	4.18	4.12	5.82
Eu	1.39	1.00	1.23	1.44	1.27	1.44	0.97	1.85
Gd	2.17	1.97	2.86	3.00	2.66	2.46	2.48	3.32
Tb	0.31	0.32	0.41	0.47	0.39	0.35	0.40	0.50
Dy	1.74	1.70	2.08	2.42	1.99	1.73	1.99	2.35
Y	7.98	8.82	10.33	12.03	10.14	8.33	10.26	10.97
Ho	0.32	0.33	0.38	0.45	0.37	0.33	0.36	0.40
Er	0.84	0.93	1.01	1.22	0.97	0.86	0.95	1.00
Tm	0.12	0.14	0.15	0.17	0.14	0.12	0.15	0.14
Yb	0.76	0.87	0.91	1.05	0.90	0.77	1.08	1.02
Lu	0.13	0.14	0.14	0.17	0.14	0.13	0.18	0.17
Th/U	2.87	3.53	3.82	3.61	3.79	3.52	4.40	4.12
Th/Ce	0.34	0.31	0.19	0.21	0.21	0.16	0.24	0.22
$^{87}Sr/^{86}Sr$	0.705651					0.706525		
$^{87}Sr/^{86}Sr_{(t)}$	0.706428					0.706427		
$^{143}Nd/^{144}Nd$	0.512461					0.512417		
$\varepsilon_{Nd(t)}$	–3.0					–4.3		
T_{DM} (Ga)	1.04					0.90		

Note: LOI—loss on ignition; T_{DM}—Nd model age.

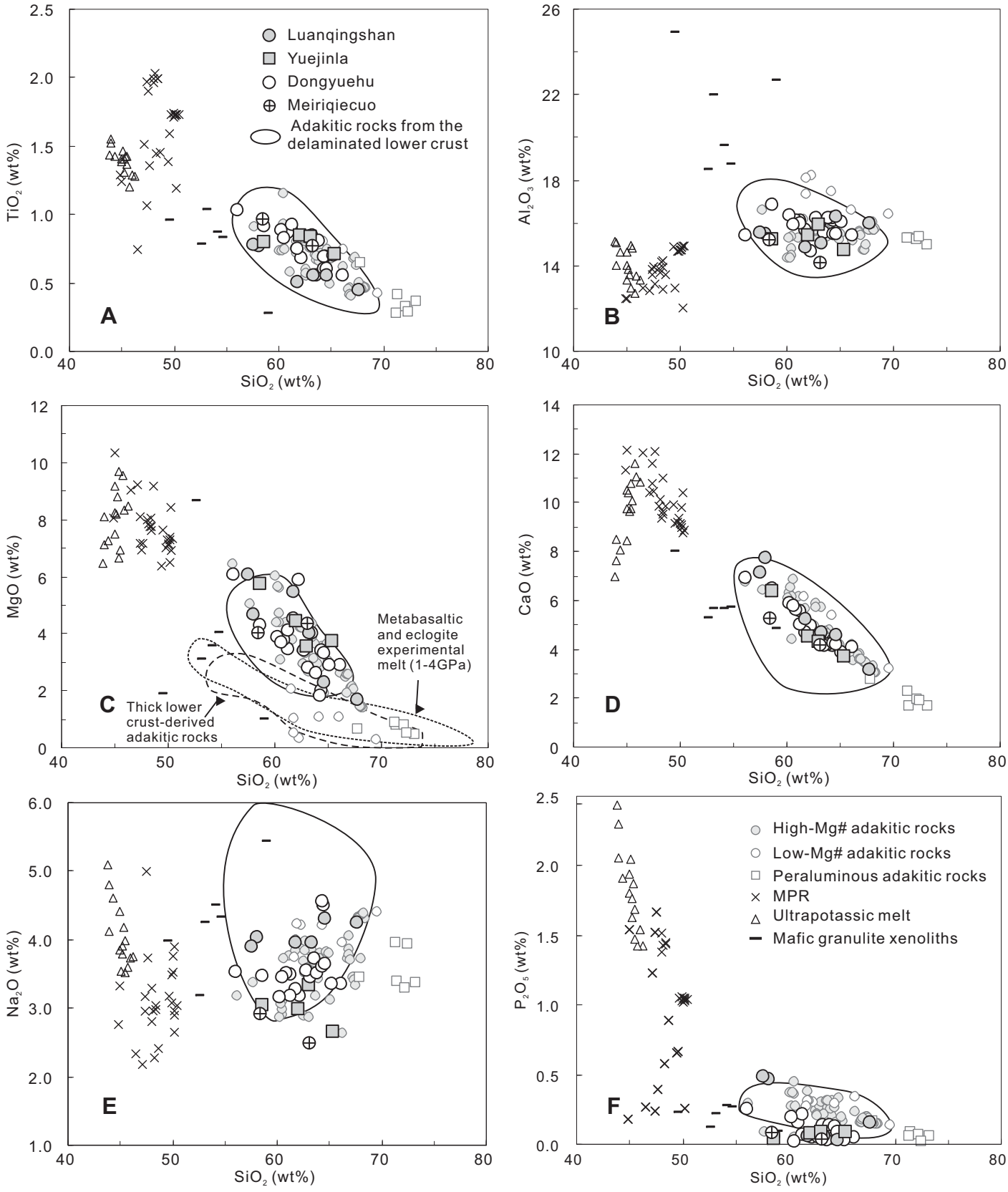

Figure 5. Harker diagrams of major-element concentrations vs. SiO_2 for Eocene adakitic rocks and other Cenozoic volcanic rocks from the Qiangtang terrane. Fields of metabasaltic and eclogitic experimental melts are after Q. Wang et al. (2006); the field of thick lower crust-derived adakitic rocks is based on Huang et al. (2009); other data sources and symbols are the same as in Figure 4. MPR—Mg-rich potassic rocks.

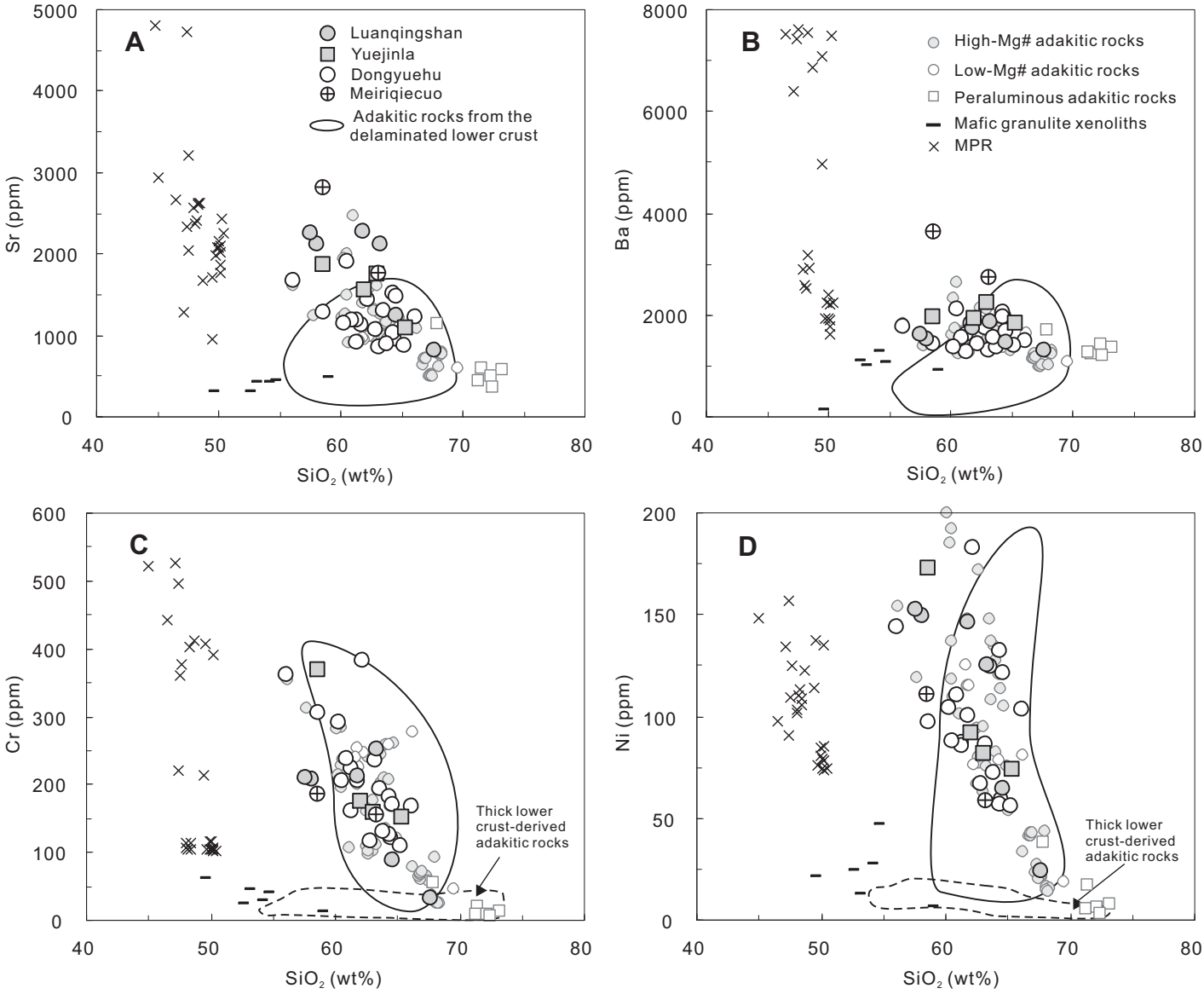

Figure 6. Plots of SiO_2 vs. trace-element concentrations for adakitic rocks and other Cenozoic volcanic rocks from the Qiangtang terrane; the field of thick lower crust–derived adakitic rocks is based on Huang et al. (2009); other data sources and symbols are the same as in Figure 4. MPR—Mg-rich potassic rocks.

Sr and Nd Isotope Geochemistry

The samples in this study have low $^{143}Nd/^{144}Nd$ ratios (0.512287–0.512461; Table 2), and negative $\varepsilon_{Nd(t)}$ values (–6.3 to –2.9; Fig. 9). They have relatively high initial $^{87}Sr/^{86}Sr_{(i)}$ ratios, ranging from 0.7062 to 0.7075 (Table 2). Their Sr and Nd isotopic compositions are different from those of Cenozoic subducted oceanic slab melts (e.g., Defant and Drummond, 1990), but they are similar to those of adakitic rocks produced during the partial melting of the lower continental crust (e.g., Petford and Atherton, 1996) and the delaminated lower continent crust in eastern China (e.g., J.F. Xu et al., 2002a; Gao et al., 2004; W.L. Xu et al., 2006). However, when compared with most mafic xenoliths, as well as Mg-rich potassic rocks from the northern Qiangtang terrane, they have higher $\varepsilon_{Nd(t)}$ values and lower $^{87}Sr/^{86}Sr_{(i)}$ ratios (Fig. 9).

DISCUSSION

Petrogenesis of Eocene High-Mg# Adakitic Rocks from the Northern Qiangtang Terrane

Eocene lavas of the northern Qiangtang terrane have features that are typical of adakitic rocks, as discussed herein. Adakite was originally defined as rocks resulting from partial melting of a young and hot subducted oceanic slab within the garnet stability field (Defant and Drummond, 1990; Martin et al., 2005). Subsequent studies have shown that adakitic rocks can also form by crustal assimilation and fractional crystallization of parental magmas of basaltic composition (AFC; Castillo et al., 1999), or partial melting of underplated or thickened crust (Atherton and Petford, 1993; Xiong et al., 2005) or delaminated lower crust (Kay and Kay, 1993; J.F. Xu et al., 2002a; Gao et al., 2004; Q. Wang et al., 2006; W.L. Xu et al., 2006).

The Qiangtang terrane is bounded by the Jinshajiang suture to the north, and the Bangong

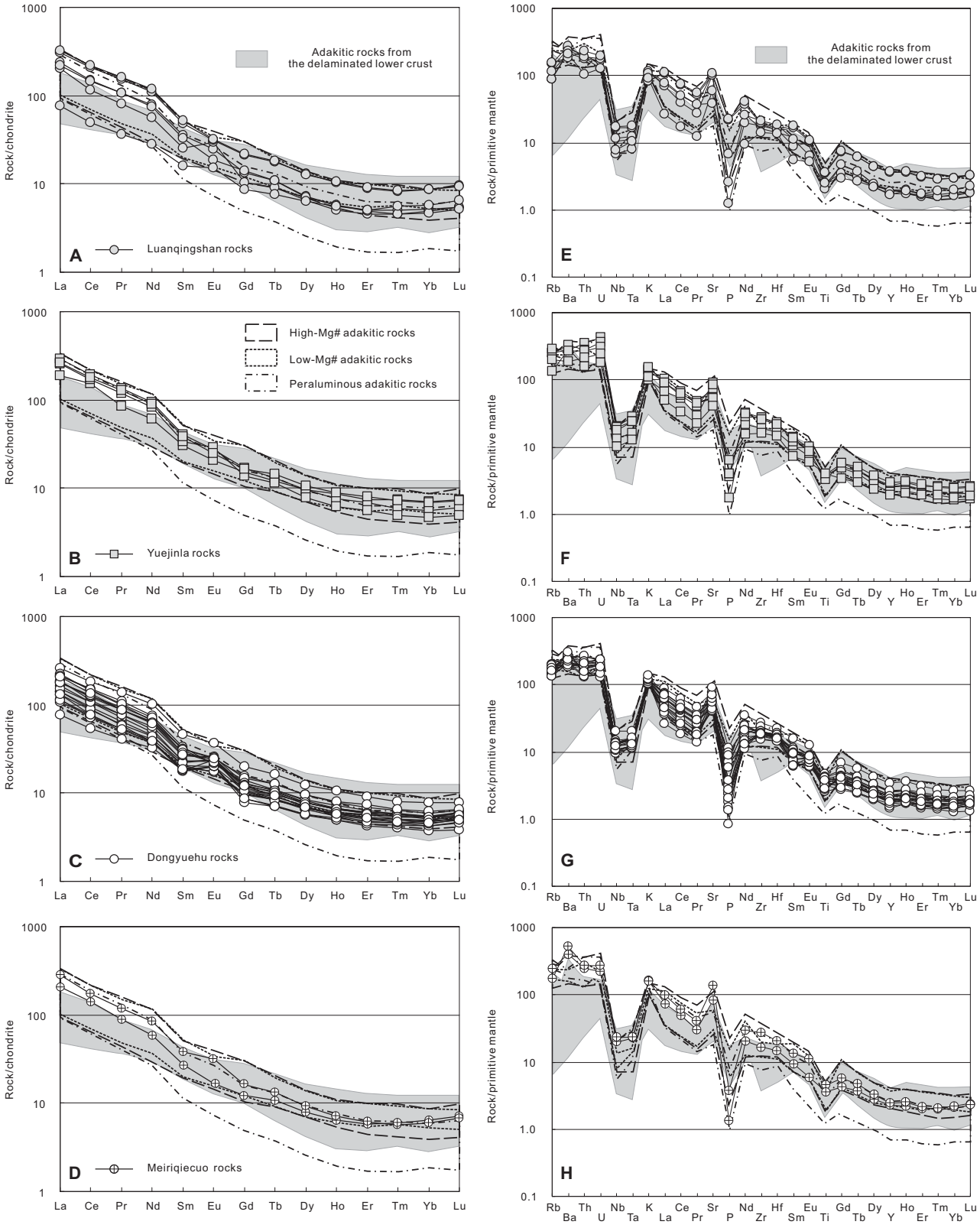

Figure 7. Chondrite-normalized rare earth element (REE) (A–D) and primitive mantle–normalized multi-element plots (E–H) for adakitic rocks of the Luanqingshan, Yuejinla, and Dongyuehu areas. Also shown are the adakitic rocks from the delaminated lower crust in eastern China (J.F. Xu et al., 2002a; Gao et al., 2004; W.L. Xu et al., 2006), and the high-Mg# adakitic rocks (Q. Wang et al., 2008; Lai and Qin, 2013), low-Mg# adakitic rocks (Lai and Qin, 2013), and peraluminous adakitic rocks (Q. Wang et al., 2008) from northern Qiangtang terrane. Normalizing values are from Sun and McDonough (1989).

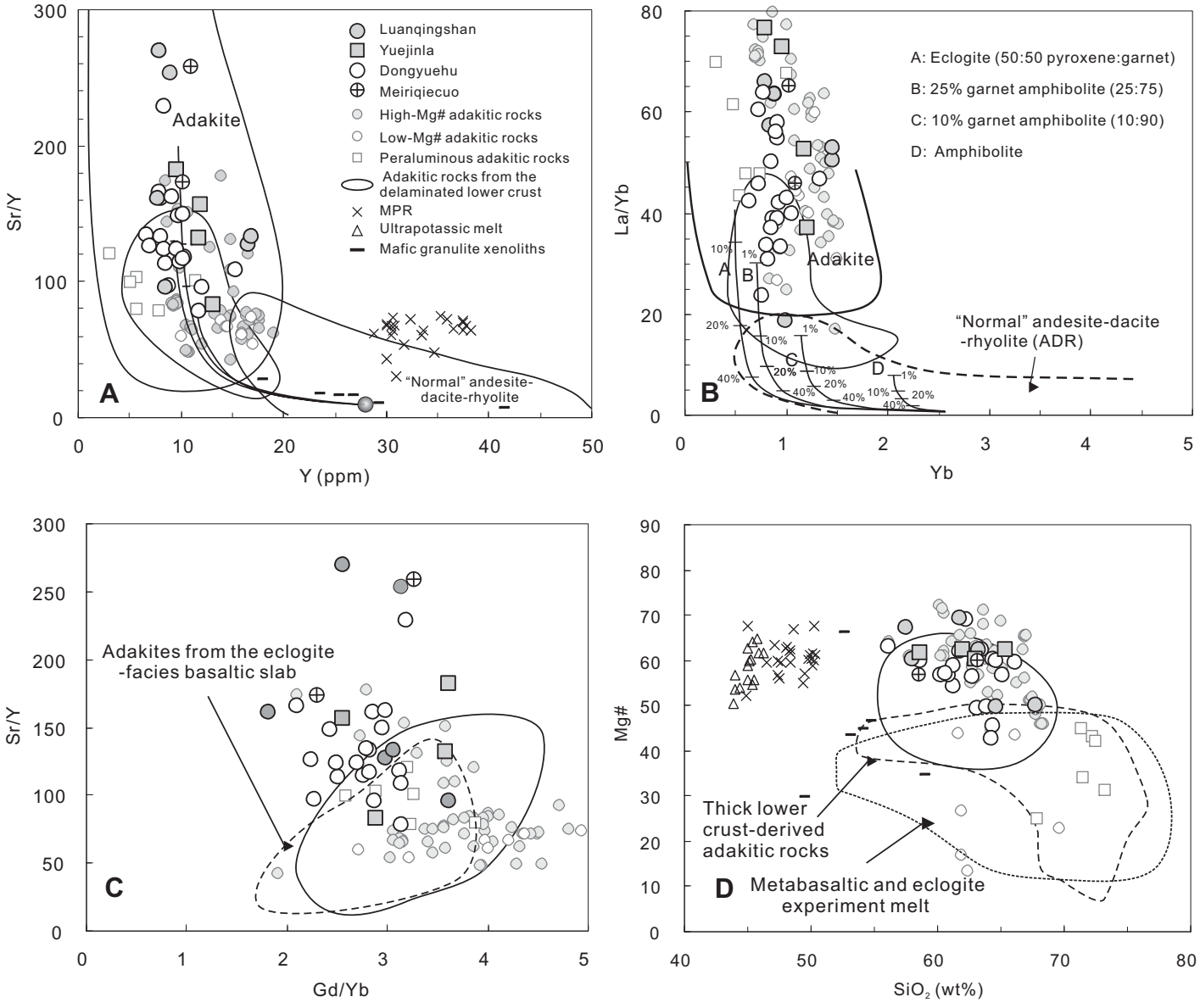

Figure 8. diagrams for adakitic rocks and other Cenozoic volcanic rocks from central Tibet: (A) Y (ppm) vs. Sr/Y, (B) Yb (ppm) vs. La/Yb (after Castillo, 2012), (C) Gd/Yb vs. Sr/Y, and (D) SiO_2 (wt%) vs. Mg# ($100 \times Mg^{2+}/[Fe^{2+} + Mg^{2+}]$). Fields of metabasaltic and eclogitic experimental melts are after Q. Wang et al. (2006); the field of thick lower crust–derived adakitic rocks is based on Huang et al. (2009); the data for adakitic rocks from the eclogite-facies basaltic slab from the central Trans-Mexican volcanic belt are from Mori et al. (2007); all other data sources and symbols are the same as in Figure 4. MPR—Mg-rich potassic rocks.

suture to the south (Yin and Harrison, 2000). It is generally accepted that suturing of the Songpan-Ganzi-Qiangtang and Qiangtang-Lhasa terranes occurred in the latest Triassic and Late Jurassic–earliest Cretaceous (Allegre et al., 1984; Chang et al., 1986; Dewey et al., 1988; Pan et al., 2012; Zhu et al., 2013), respectively. It therefore follows that the northern Qiangtang terrane has been in an intracontinental setting since the Late Triassic (Pan et al., 2012). Recent studies of the large-scale Early Tertiary volcanic rocks (e.g., Lee et al., 2009, 2012) and mafic dikes (e.g., Gao et al., 2008; Y.G. Xu et al., 2008) in southern Tibet imply that the Neotethyan slab broke off during the Eocene. In addition, geophysical evidence (Owens and Zandt, 1997; Tilmann et al., 2003) indicates that the northward-subducted Indian plate and Tethyan oceanic slabs have not reached the southern boundary of the Qiangtang terrane (Bangong suture), suggesting that there was no subducted oceanic slab beneath the Qiangtang terrane (Liu et al., 2008; Q. Wang et al., 2008). Tomographic imaging of the mantle under Tibet reveals a possible presence of Tethyan oceanic crust beneath the central Tibet (van der Voo et al., 1999). It is possible that this fossil oceanic slab melted and then reacted with surrounding mantle peridotites to produce the adakitic rocks in this study. However, compared with the typical adakites with mid-ocean-ridge basalt (MORB)–like Sr-Nd isotopic compositions ($^{87}Sr/^{86}Sr_{[i]} < 0.7045$, $\varepsilon_{Nd[t]} > 0$), and relatively low K_2O (<3 wt%) and low Th contents (Defant and Drummond, 1990; Kelemen et al., 2003; Plank, 2005; Xiong et al., 2006), pro-

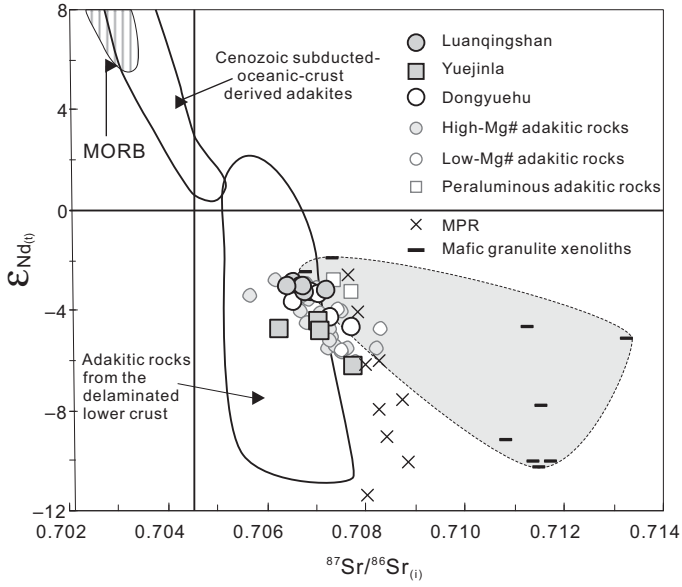

Figure 9. $^{87}Sr/^{86}Sr_{(i)}$ vs. $\varepsilon_{Nd(t)}$ diagram for adakitic rocks, and other Cenozoic volcanic rocks from the northern Qiangtang terrane. MORB—mid-ocean-ridge basalt data are from Niu and Batiza (1997), whereas the data for Cenozoic subducted-oceanic-crust–derived adakitic rocks are after Defant et al. (1992), Kay and Kay (1993), and Stern and Kilian (1996). The data for xenoliths from Cenozoic volcanic rocks of the Qiangtang terrane are from Deng et al. (1998) and Lai and Qin (2008). All other data sources and symbols are the same as in Figure 4. MPR—Mg-rich potassic rocks.

duced by partial melting of subducting slabs in modern arcs, the adakitic rocks described in this study have relatively high K_2O (2.46–4.85 wt%) and Th (8.7–29.0 ppm) contents (Table 2), low $\varepsilon_{Nd(t)}$ values (–6.3 to –2.9), and high $^{87}Sr/^{86}Sr_{(i)}$ ratios (0.7062–0.7075) (Fig. 9), which clearly distinguish them from the adakites derived from the partial melting of a subducted oceanic slab. Moreover, the Eocene rocks from northern Tibetan Plateau have Nb/U, Ce/Pb, Ti/Eu, and Nd/Sm ratios differing from that of MORB but resembling the crustal values (Fig. 10), further strengthening their continental affinity. Thus, it is unlikely that the Eocene adakitic rocks from the northern Qiangtang terrane were produced by partial melting of a subducted oceanic slab.

The second possible origin of the adakitic rocks of this study is a mantle-derived basaltic magma modified by crustal assimilation and fractional crystallization (AFC) processes. However, this hypothesis is inconsistent with the following field observations and geochemical features for these rocks: (1) Mafic and ultramafic lavas have not been found in or around the present study area. (2) The lack of significant negative Eu and Sr anomalies in measured samples indicates that the magmas did not form from a mafic or ultramafic melt by extended fractional crystallization of plagioclase at crustal levels (Fig. 7). (3) If adakitic magmas in this study were produced by AFC, the value of La/Yb should be invariable or increasing when the Mg# number decreases, but this relationship is not shown on the plot of $Mg^{\#}$ versus La/Yb (Fig. 11A). (4) Given the high content of Zr (or Th) in the crust and its compatible character in evolved rocks, when SiO_2 contents increase, the content of Zr (or Th) should increase, but such a relationship is not evident in the plot of SiO_2 versus Zr (or Th) (Figs. 11B and 11C). Finally, (5) the positive correlation of 1000/Sr versus $^{87}Sr/^{86}Sr_{(i)}$ is not consistent with AFC (Fig. 11D).

Recently, Q. Wang et al. (2008, 2010) suggested that the high-Mg# adakitic rocks from the northern Qiangtang terrane originated from interaction between the mantle and sediment-dominated continental-crust–derived melts of the south-dipping Songpan-Ganzi terrane along the Jinshajiang suture. This hypothesis, however, is inconsistent with the following observations: (1) The lavas in the northern Qiangtang terrane were emplaced in a planar

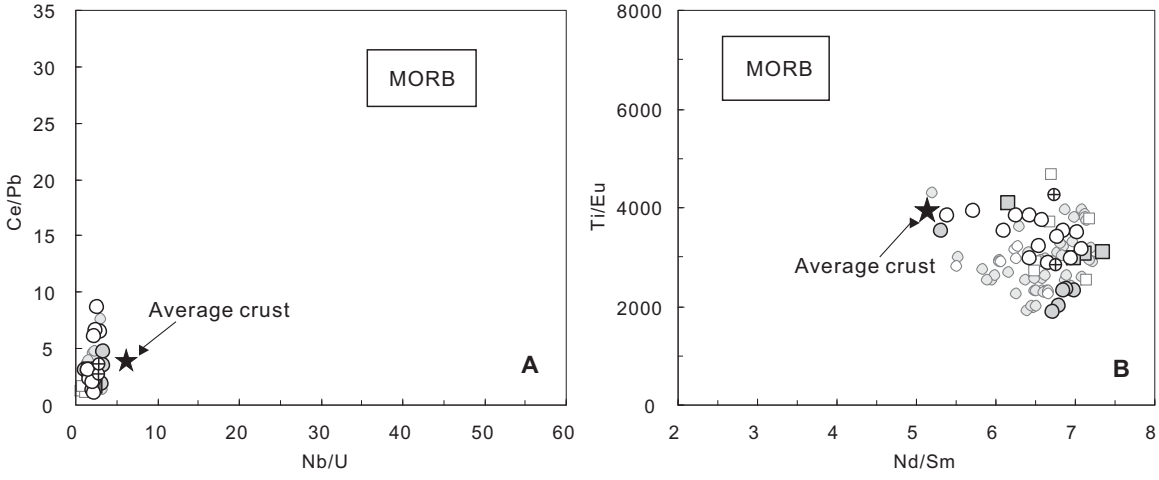

Figure 10. Plots of (A) Nb/U vs. Ce/Pb and (B) Nd/Sm vs. Ti/Eu for adakitic rocks from the northern Qiangtang terrane. Field of mid-ocean-ridge basalt (MORB) is from Klein (2003), the average crust is from Rudnick and Gao (2003), and other data sources and symbols are the same as in Figure 4.

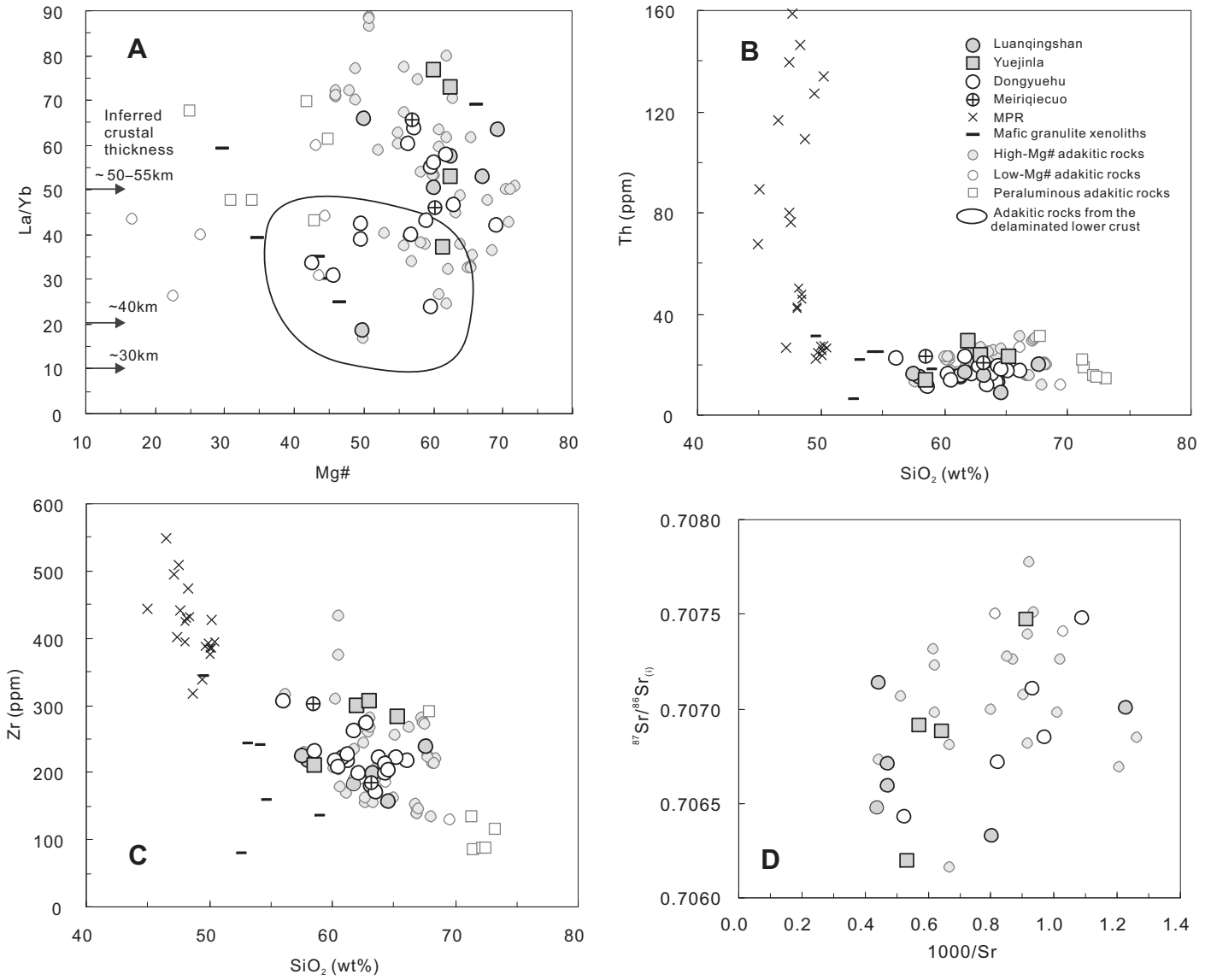

Figure 11. Plots of (A) Mg# vs. La/Yb, (B) Th vs. SiO_2, (C) Zr vs. SiO_2, and (D) $^{87}Sr/^{86}Sr_{(i)}$ vs. 1000/Sr for high-Mg# adakitic rocks and other Cenozoic volcanic rocks from the Qiangtang terrane; data sources and symbols are the same as in Figure 4. MPR—Mg-rich potassic rocks.

spread instead of in an E-W linear orientation. (2) Adakitic rocks are commonly formed in extensional tectonic settings rather than compressional tectonic environments (J.F. Xu et al., 2002a; Gao et al., 2004; Q. Wang et al., 2006, 2008), but the Eocene north-south–oriented dikes throughout central Tibet indicate that an E-W extensional tectonic setting existed at that time (Q. Wang et al., 2010). (3) It is difficult for buoyant sediment-dominated continental crust to enter the deep mantle via continental subduction. (4) If the lower crust beneath the northern Qiangtang terrane was made of hydrated basaltic rocks from Jinshajiang oceanic lithosphere by southward subduction since late Mesozoic time (Kapp et al., 2000), there should be a cold, high-velocity crust beneath the northern Qiangtang block; however, present geophysical data indicate that it may be composed by hot felsic components (e.g., Galve et al., 2006), and the magnetotelluric data (e.g., Unsworth et al., 2004) and the seismic researches (e.g., Owens and Zandt, 1997) indicate that Asian lithosphere extends as far south as the Kunlun Shan. (5) The results of tomography conducted by Zhou and Murphy (2005) hint that the southward subduction of Asian continental crust did not take place beneath the northern Qiangtang terrane.

Experimental results indicate that when melts interact with mantle peridotite, their Mg# can be elevated significantly (Rapp and Watson, 1995; Rapp et al., 1999). The adakitic rocks of this study have distinctly higher MgO (1.67–6.07 wt%), Cr (34–382 ppm), and Ni (24–183 ppm) contents and higher Mg# (43–69) than the adakitic rocks derived from underplated or thickened lower crust (Figs. 5C, 6C, 6D, and 8D), implying that they were generated with the involvement of a mantle component. Meanwhile, the adakitic rocks also show a continental crust affinity, such as high K_2O and Th contents, high Th/Ce ratios (0.12–0.35), and low Nb/U, Ce/Pb, Ti/Eu, and Nd/Sm ratios (Fig. 10) (Rapp et al., 2003; Q. Wang et al., 2005, 2006; Rudnick and Gao, 2003). In addition, a plot of Sr and Nd isotope ratios falls within the region of garnet-bearing amphibolite xenoliths from Cenozoic volcanic rocks from the Qiangtang terrane (Deng et al., 1998; Lai and

Qin, 2008) (Fig. 9). We therefore favor the model whereby the eclogitic lower crust, together with the underlying lithospheric mantle, was delaminated. The delaminated lower crust melted as it was heated by upwelling asthenospheric mantle, and such a melt interacted with surrounding mantle peridotites during its ascent, resulting in similar geochemical characteristics as the adakitic rocks produced by partial melting of delaminated garnet-bearing lower continental crust in eastern China. This hypothesis is consistent with the following observations: (1) The high-Mg# adakitic rocks have a clear continental crust affinity, such as high K_2O and Th contents, high Th/Ce ratios (0.12–0.35), and low Nb/U, Ce/Pb, Ti/Eu, and Nd/Sm ratios (Fig. 10), as well as low $^{143}Nd/^{144}Nd_{(t)}$ and high $^{87}Sr/^{86}Sr_{(i)}$ isotopic ratios (Fig. 9). (2) The Th content and Th/La ratio of high-Mg# adakitic rocks are similar to the mafic xenoliths in the Cenozoic lavas from the northern Qiangtang terrane (Fig. 11B) (Lai and Qin, 2008, 2013). (3) The existence of some olivine xenocrysts in the high-Mg# samples clearly suggests that the primary adakitic melts captured some olivine crystals during their ascent process (Lai and Qin, 2013). (4) A high-velocity layer in the lower crust characteristic of mafic rocks is absent in the northern Qiangtang terrane (e.g., Galve et al., 2006). (5) The delamination of lower crust of the northern Qiangtang terrane caused the upwelling asthenospheric mantle, which could have led to the high temperatures beneath the northern Tibetan Plateau (e.g., Owens and Zandt, 1997; Alsdorf and Nelson, 1999; Hacker et al., 2000; Zhou and Murphy, 2005), triggering the crustal weakening and eastward escape of deep crust in central Tibet (e.g., Royden et al., 1997, 2008; Clark and Royden, 2000; Klemperer, 2006; Zhang et al., 2010).

To evaluate this hypothesis, we investigated a simple two-member mixing process, and the results are shown in Figure 12. The modeling shows that the addition of less than 10% mantle olivine (Fo_{90}) to melts derived from mafic granulite (Fig. 12A), metabasalt, or eclogite at 1.0–3.2 GPa (Fig. 12B) could consistently produce the Nb/U values and isotopic characteristics observed in the high-Mg# adakitic rocks.

In conclusion, partial melting of a delaminated lower crust in the presence of residual garnet + rutile and amphibole (but not plagioclase), followed by reaction with mantle peridotites during ascent, can explain the formation of the high-Mg# adakitic rocks from the study area.

Relationship between Eocene Mantle-Derived Mg-Rich Potassic Rocks and High-Mg# Adakitic Rocks

Eocene Mg-rich potassic rocks (with MgO ≥ 6 wt% and $K_2O/Na_2O > 1$; i.e., of the shoshonitic series) have been found in the northern Qiangtang terrane (e.g., Deng, 1998; Williams et al., 2004; Guo et al., 2006; Chen et al., 2012), associated with the high-Mg# adakitic rocks described in this study. The Mg-rich potassic rocks have high concentrations of MgO, Ni, and Cr (Figs. 5C, 6c, and 6D), indicating they formed from a nearly primitive magma that experienced only minimal crustal contamination (Williams et al., 2004; Guo et al., 2006; Chen et al., 2012). They have geochemical characteristics typical of rocks derived from an enriched mantle source, such as relatively high $^{87}Sr/^{86}Sr_{(i)}$ ratios and low $\varepsilon_{Nd(t)}$ values (Fig. 9), as well as high concentrations of K_2O (Fig. 4B) and other LILEs (Fig. 6A and 6B), and a depletion in HFSEs (not shown).

If the Mg-rich potassic rocks did indeed originate from an enriched mantle, their melts may have evolved to the high-Mg# adakitic rocks. For example, Holbig and Grove (2008) recently suggested that Cenozoic K-rich rocks from Tibet were produced by fractional crystallization of a mantle melt that originated within the lithospheric mantle or lower continental crust. However, compared with experimental studies (Holbig and Grove, 2008) and mantle-derived Mg-rich potassic rocks from the northern Qiangtang terrane, the high-Mg# adakitic rocks of this study exhibit major-element (such as K_2O and Na_2O; Figs. 4B and 5E) and incompatible-element concentrations (such as Ba, Rb,

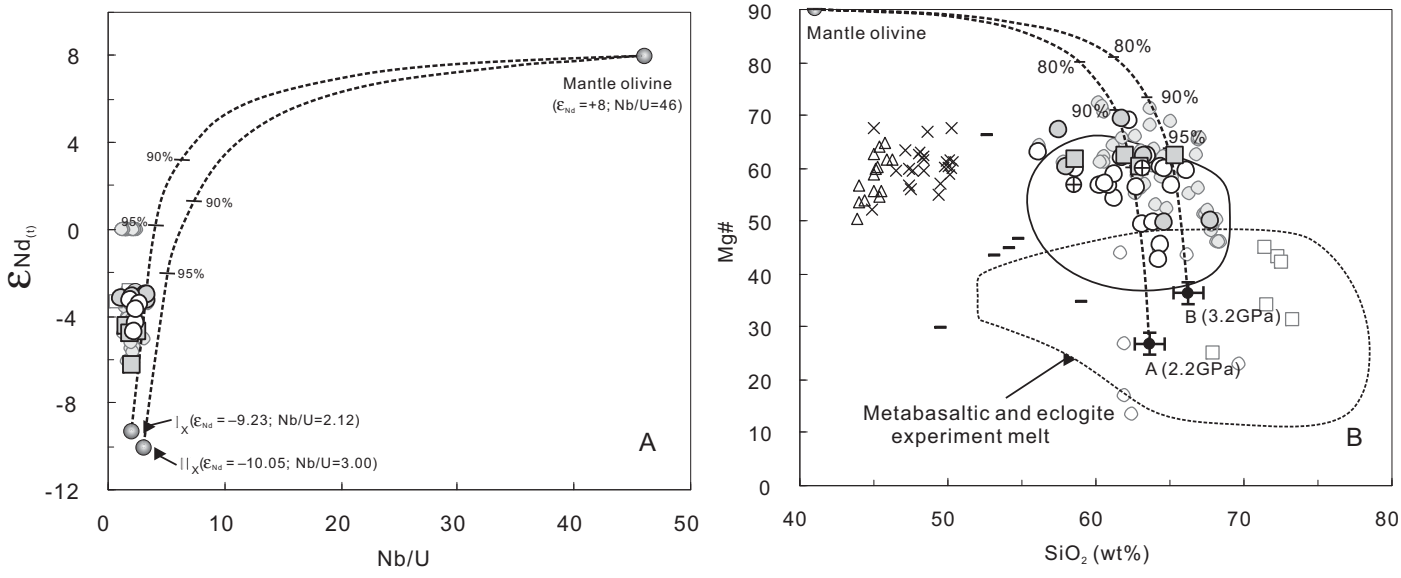

Figure 12. Geochemical modeling of the mixing between mantle olivine and melts derived from mafic granulite, metabasalt, or eclogite, based on (A) Nb/U vs. $\varepsilon_{Nd(t)}$ and (B) a plot of SiO_2 and Mg# values. The modeling results show that the addition of less than 10% mantle olivine (Fo_{90}) to melts derived from the mafic granulite (Fig. 11a), metabasalt, or eclogite at 1.0–3.2 GPa could consistently explain the Nb/U values, Mg#, and isotopic characteristics observed in the high-Mg# adakitic rocks. Data sources: mafic granulite xenoliths from Cenozoic volcanic rocks in Qiangtang terrane (I_X and II_X) are from Lai and Qin (2008); experimental metabasaltic/eclogite melts (1–4 GPa) are from Rapp et al. (1999) and references therein. Melt A: *P* = 2.2 GPa, *T* = 1075 °C, residue = clinopyroxene (Cpx) + garnet (Gt) (Rapp and Watson, 1995). Melt B: *P* = 3.2 GPa, *T* = 1100 °C, residue = Cpx + Gt (Rapp et al., 1999).

and Sr; Figs. 6A and 6B) that do not support this hypothesis. Similarly, there are not appropriate trends on plots of Mg# versus La/Yb, SiO_2 versus Th, SiO_2 versus Zr, and $^{87}Sr/^{86}Sr_{(i)}$ versus 1000/Sr, as discussed earlier herein (Figs. 11A–11D). Thus, we do not consider the high-Mg# adakitic rocks to be the product of evolved Mg-rich potassic magmas from the northern Qiangtang terrane.

Considering the absence of a high-velocity layer in the lower crust (e.g., Galve et al., 2006), as well as the presence of contemporary high-Mg# adakitic rocks, we suggest that the Eocene Mg-rich potassic rocks and other coeval rocks, such as shoshonitic rocks and diabase dikes (e.g., Q. Wang et al., 2010), from the northern Qiangtang terrane were derived from enriched mantle, most likely triggered by the delamination of lithospheric mantle.

Implications for Regional Tectonic Evolution

Although much of the Tibetan Plateau is flat, with an average elevation of 5 km (Fielding et al., 1994), and a crust approximately twice as thick as elsewhere (Molnar, 1988), the questions of how and when such a thick crust was generated remain controversial, especially whether there was an early plateau uplifting at ca. 40 Ma (Chung et al., 1998, 2005; C. Wang et al., 2008; Li et al., 2012; Rohrmann et al., 2012). So far, the most prominent models are those of convective removal (Turner et al., 1993, 1996; Chung et al., 1998; Williams et al., 2001) and of intracontinental subduction (Roger, et al., 2000; Tapponnier et al., 2001; Ding et al., 2003, 2007; Guo et al., 2006; Q. Wang et al., 2008b, 2010).

Turner et al. (1993, 1996) argued that convective removal of the lower lithosphere is the mechanism most likely to have triggered the Cenozoic petrogenesis of postcollisional lavas in Tibet. However, the time scale of convective thinning is not greater than ~5 m.y., which is considerably shorter than the ranges of semicontinuous postcollisional magmatism in northern and southern Tibet during the Cenozoic (Williams et al., 2004; Guo et al., 2006). On the other hand, the spatiotemporal distribution of high-Mg potassic rocks and other Cenozoic lavas and associated topographic uplift of the Tibetan Plateau have been regarded as the integrated effect of multiple tectonic events (Williams et al., 2004; Xia et al., 2011; Chen et al., 2012).

Subsequently, based on the distribution of some volcanic rocks along the margins of the east-west–trending tectonic belts and seismic studies, Tapponnier et al. (2001) suggested that the uplift of Tibet developed by stepwise growth involving north- and south-directed intracontinental subduction. However, Williams et al. (2004) suggested that the processes of oblique continental subduction would not have supplied sufficient heat to generate the high geothermal gradients observed in southern and northern Tibet. In addition, Tibetan Cenozoic volcanic rocks are also found within the hinterland of each terrane, e.g., the potassic-ultrapotassic rocks in the midwestern part of the Lhasa terrane (e.g., Williams et al., 2004; Chen et al., 2006; Ding et al., 2006; Zhao et al., 2009b) and the central Qiangtang terrane (Zhao et al., 2009a). Moreover, this model cannot explain the high MgO, Cr, and Ni contents of the high-Mg# adakitic rocks in this study.

C. Wang et al. (2008) suggested that the central plateau was at or near its modern elevation by 40 Ma on the basis of geological and geophysical data, and Spurlin et al. (2005), Aikman et al. (2008), Li et al. (2012), Rohrmann et al. (2012), and Q. Xu et al. (2013) proposed that crustal thickening began in central Tibet during the Eocene based on tectonic and basin analysis. Those studies suggested that there was early elevation in central Tibet. Recent experimental results suggest that the adakitic melts can generally be produced from material at pressures equivalent to a crustal thickness of >50 km, where the residual phases include garnet ± rutile but little or no plagioclase (Rapp et al., 1999, 2003; Xiong et al., 2005; Xiao and Clemens, 2007). Therefore, the occurrence of adakitic magmatism in the northern Qiangtang terrane indicates the presence of a thickened eclogitic lower crust at ca. 46 Ma, implying that significant early uplift of the central plateau occurred between 46 and 38 Ma (e.g., Dong et al., 2008; Liu et al., 2008; Q. Wang et al., 2008, 2010; Chen et al., 2012). In addition, the broad distribution of north-south–trending Eocene dikes in the Qiangtang terrane indicates an extensional tectonic setting between 47 and 38 Ma (e.g., Yin et al., 1999; Blisniuk et al., 2001; Q. Wang et al., 2010; Rohrmann et al., 2012). As such, we suggest that the thickened lower crust in central Tibet (northern Qiangtang terrane) is most likely to have delaminated during the Eocene.

Bird (1979) suggested that the Tibetan Plateau was formed by delamination of the entire continental lithospheric mantle, which was replaced by hot asthenosphere that came into direct contact with the base of the crust. However, considering the sparsity of Eocene mafic lavas, the fact that mantle-derived Mg-rich potassic rocks and shoshonitic rocks are only found in a few areas (such as the Bangdacuo area; Deng, 1998; Ding et al., 2003; Williams et al., 2004; Guo et al., 2006), and the distribution of high-Mg# adakitic rocks, which are predominantly in the midwest of the northern Qiangtang terrane, we interpret that the lower crust was not extensively delaminated into deeper convecting mantle beneath the Tibetan Plateau. We suggest that the Eocene delamination of the thickened lower crust only took place below the midwestern region of the northern Qiangtang terrane, and that the partial melts, formed from the delaminated lower crust, subsequently reacted with the surrounding mantle peridotites during ascent to crustal depths, resulting in the formation of the high-Mg# adakitic rocks.

Based on this study, and combined with regional evolution, and an Early Tertiary tectono-magmatic evolution model for the northern Qiangtang terrane, central Tibet is summarized as follows:

(1) Before the Cenozoic (>60 Ma) (Fig. 13A), following the complete closure by northern subduction of the Neotethys and Midtethys Oceans, the Lhasa and Qiangtang terrane was in an intracontinental setting. Under compressive stress, the continental crust of the Qiangtang terrane was probably of a normal thickness, was subjected to weak deformation, and began to be thickened.

(2) During the Paleocene and early Eocene (60–46 Ma) (Fig. 13B), in response to the India-Asia collision at 65–55 Ma, the upper continental crust was tectonically piled, leading to gradual thickening of the entire lithosphere in the northern Qiangtang terrane. This process led to the upper-crustal shortening and the lower-crustal basaltic/gabbroic protoliths transformed to amphibolite to granulite-eclogite-garnet clinopyroxenite assemblages at high pressure (Rapp and Watson, 1995).

(3) Due to the increase in density and gravitational instability, the lower crust and lithospheric mantle probably sank into the asthenospheric mantle during the Eocene (ca. 46–38 Ma) beneath the midwestern region of the northern Qiangtang terrane (Fig. 13C). This delamination would have induced the upwelling of hot asthenospheric mantle, as well as rapid uplift of the center of the Tibetan Plateau. Upwelling asthenospheric material triggered dehydration melting of delaminated lower crust (amphibole- and ecologite-bearing crust) and enriched lithospheric mantle. The former reacted with the surrounding mantle peridotite to form the high-Mg# adakitic magmas, while the latter produced the Mg-rich potassic and shoshonitic magmas in the northern Qiangtang terrane. A regional steepening of the geothermal gradient, triggered by uprising of the asthenosphere, combined with decompression induced by E-W extension, led to partial melting of the mafic material beneath the crust, thereby generating the magmas that would subsequently form the low-Mg# adakitic

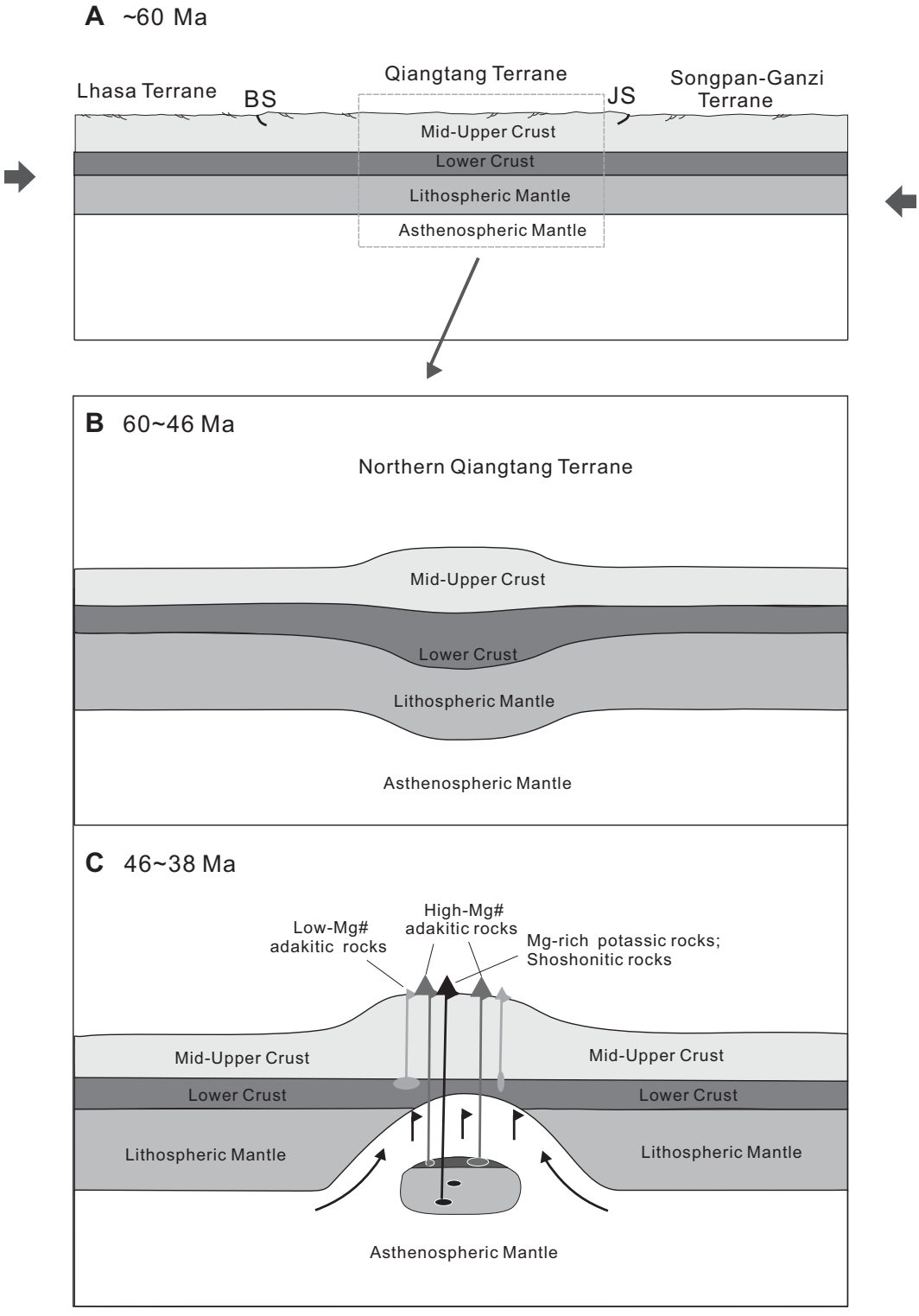

Figure 13. Simplified model of the generation of Eocene high- and low-Mg# adakitic rocks, and mantle-derived Mg-rich potassic rocks, from the mid-western region of the northern Qiangtang terrane. BS—Bangong suture; JS—Jinshajiang suture.

rocks found in the northern Qiangtang terrane (e.g., Q. Wang et al., 2008; Lai and Qin, 2013; Lai and Qin, 2013). These magmas rose to the surface via extensional structures and structural weaknesses in the overlying tectonic belts to form the low-Mg#, and high-Mg# adakitic rocks and andesitic dikes (Lai et al., 2003; Lai and Qin, 2013; Liu et al., 2008; Dong et al., 2008; C. Wang et al., 2008; Q. Wang et al., 2010; B.D. Wang et al., 2010), Mg-rich potassic rocks, and other shoshonitic rocks or dikes (Turner et al., 1996; Deng, 1998; Ding et al., 2003, 2007; Williams et al., 2004; Guo et al., 2006; Q. Wang et al., 2010).

CONCLUSION

The widespread Eocene magmatism in the northern Qiangtang terrane indicates a significant tectonothermal event that occurred in a postcollision setting. Geochronological and geochemical data of Eocene volcanic rocks

reported in this paper, combined with the data in the literature, yielded the following conclusions:

(1) The lavas in the northern Qiangtang terrane, central Tibet, have adakite-like major- and trace-element features, such as high SiO_2, Al_2O_3, and Sr contents, and high Sr/Y and La/Yb ratios, but low Y and Yb contents, combining with high Mg# (43–69) and high Cr and Ni contents. The presence of Eocene adakitic rocks suggests that the crustal thickness in northern Qiangtang terrane was at least 50 km at ca. 46 Ma.

(2) The Eocene high-Mg# adakitic rocks from the northern Qiangtang terrane show a clear continental crust affinity, such as high K_2O and Th contents, high Th/Ce ratios, and low Nb/U, Ce/Pb, Ti/Eu, and Nd/Sm ratios, as well as low $\varepsilon_{Nd(t)}$ and high $^{87}Sr/^{86}Sr_{(i)}$ values. It is probable that they were produced by dehydration melting of delaminated lower crust, followed by interaction with the surrounding mantle.

(3) The broad outcrop of high-Mg# adakitic rocks with ages of 46–38 Ma in the northern Qiangtang terrane, coupled with contemporary mantle-derived Mg-rich potassic lavas, shoshonitic lavas, and N-S–oriented dikes with ages of 47–38 Ma, indicates an early period of rapid uplift and extension, most likely caused by small-scale delamination of the lithospheric mantle beneath the central Tibetan Plateau.

ACKNOWLEDGMENTS

This research was supported by the following funding agencies: the Natural Science Foundation of China (40930316, 40872055), the Major State Basic Research Program of the People's Republic of China (2009CB421004, 2011CB403100), the Strategic Priority Research Program(B) of the Chinese Academy of Sciences (XDB03010300), the International Geoscience Correlation Programme (IGCP) project (IGCP/SIDA-600), and the China Geological Survey (1212010818098). This is contribution No. IS-1704 from GIGCAS.

REFERENCES CITED

Aikman, A.B., Harrison, T.M., and Ding, L., 2008, Evidence for early (>44 Ma) Himalayan crustal thickening, Tethyan Himalaya, southeastern Tibet: Earth and Planetary Science Letters, v. 274, p. 14–23, doi:10.1016/j.epsl.2008.06.038.

Allegre, C.J., Courtillot, V., Tapponnier, P., Hirn, A., Mattauer, M., Coulon, C., Jaeger, J.J., Achache, J., Scharer, U., Marcoux, J., Burg, J.P., Girardeau, J., Armijo, R., Gariepy, C., Gopel, C., Li, T.D., Xiao, X.C., Chang, C.F., Li, G.Q., Lin, B.Y., Teng, J.W., Wang, N.W., Chen, G.M., Han, T.L., Wang, X.B., Den, W.M., Sheng, H.B., Cao, Y.G., Zhou, J., Qiu, H.R., Bao, P.S., Wang, S.C., Wang, B.X., Zhou, Y.X., and Xu, R.H., 1984, Structure and evolution of the Himalaya-Tibet orogenic belt: Nature, v. 307, p. 17–22, doi:10.1038/307017a0.

Alsdorf, D., and Nelson, D., 1999, Tibetan satellite magnetic low: Evidence for widespread melt in the Tibetan crust: Geology, v. 27, p. 943–946, doi: 10.1130/0091-7613(1999)027<0943:TSMLEF>2.3.CO;2.

Atherton, M.P., and Petford, N., 1993, Generation of sodium-rich magmas from newly underplated basaltic crust: Nature, v. 362, p. 144–146, doi:10.1038/362144a0.

Bird, P., 1979, Continental delamination and the Colorado Plateau: Journal of Geophysical Research, v. 84, no. B13, p. 7561–7571, doi:10.1029/JB084iB13p07561.

Blisniuk, P.M., Hacker, B.R., Glodny, J., Ratschbacher, L., Bi, S., Wu, Z., McWilliams, M.O., and Calvert, A., 2001, Normal faulting in central Tibet since at least 13.5 Myr ago: Nature, v. 412, p. 628–632, doi:10.1038/35088045.

Castillo, P.R., 2012, Adakite petrogenesis: Lithos, v. 134–135, p. 304–316, doi:10.1016/j.lithos.2011.09.013.

Castillo, P.R., Janney, P.E., and Solidum, R.U., 1999, Petrology and geochemistry of Camiguin island, southern Philippines: Insights to the source of adakites and other lavas in a complex arc setting: Contributions to Mineralogy and Petrology, v. 134, p. 33–51, doi:10.1007/s004100050467.

Chang, C.F., Chen, N.S., Coward, M.P., Deng, W.M., Dewey, J.F., Gansser, A., Harris, N.B.W., Jin, C.W., Kidd, W.S.F., Leeder, M.R., Li, H., Lin, J.L., Liu, C.J., Mei, H.J., Molnar, P., Pan, Y., Pan, Y.S., Pearce, J.A., Shackleton, R.M., Simth, A.B., Sunm, Y.Y., Ward, M., Watts, D.R., Xu, J.T., Xu, R.H., Yin, J.X., and Zhang, Y.Q., 1986, Preliminary conclusion of the Royal Society and Academia Sinica 1985 geotraverse of Tibet: Nature, v. 323, p. 501–507, doi:10.1038/323501a0.

Chen, J.L., Xu, J.F., Kang, Z.Q., and Wang, B.D., 2006, Origin of the Miocene Bugasi group volcanic rocks in the Cuoqin County, western Tibetan Plateau: Acta Petrolei Sinica, v. 22, p. 585–594.

Chen, J.L., Xu, J.F., Wang, B.D., Kang, Z.Q., and Li, J., 2010, Origin of Cenozoic alkaline potassic volcanic rocks at KonglongXiang, Lhasa terrane, Tibetan Plateau: Products of partial melting of a mafic lower-crustal source: Chemical Geology, v. 273, p. 286–299, doi:10.1016/j.chemgeo.2010.03.003.

Chen, J.L., Xu, J.F., Wang, B.D., and Kang, Z.Q., 2012, Cenozoic Mg-rich potassic rocks in the Tibetan Plateau: Geochemical variations, heterogeneity of subcontinental lithospheric mantle and tectonic implications: Journal of Asian Earth Sciences, v. 53, p. 115–130, doi:10.1016/j.jseaes.2012.03.003.

Chi, X.G., Li, C., Wei, J., Liu, S., and Yang, R.H., 1999, Spatial-temporal time evolution of Cenozoic volcanism and uplift in northern Tibet: Geological Review, v. 45, p. 978–986.

Chung, S.L., Lo, C.H., Lee, T.Y., Zhang, Y., Xie, Y., Li, X., Wang, K.L., and Wang, P.L., 1998, Diachronous uplift of the Tibetan Plateau starting 40 Myr ago: Nature, v. 394, p. 769–773, doi:10.1038/29511.

Chung, S.L., Liu, D., Ji, J., Chu, M.F., Lee, H.Y., Wen, D.J., Lo, C.H., Lee, T.Y., Qian, Q., and Zhang, Q., 2003, Adakite from continental collision zones: Melting of thickened lower crust beneath southern Tibet: Geology, v. 31, p. 1021–1024, doi:10.1130/G19796.1.

Chung, S.L., Chu, M.F., Zhang, Y.Q., Xie, Y., Lo, C.H., Lee, T.Y., Lan, C.Y., Li, X., Zhang, Y.Q., and Wang, Y., 2005, Tibetan tectonic evolution inferred from spatial and temporal variations in post-collisional magmatism: Earth-Science Reviews, v. 68, p. 173–196, doi:10.1016/j.earscirev.2004.05.001.

Clark, M.K., and Royden, L.H., 2000, Topographic ooze: Building the eastern margin of Tibet by lower crustal flow: Geology, v. 28, p. 703–706, doi:10.1130/0091-7613(2000)28<703:TOBTEM>2.0.CO;2.

Coldwell, B., Clemens, J., and Petford, N., 2011, Deep crustal melting in the Peruvian Andes: Felsic magma generation during delamination and uplift: Lithos, v. 125, p. 272–286, doi: org/10.1016/j.lithos.2011.02.011.

Condie, K.C., 2005, TTGs and adakites: Are they both slab melts: Lithos, v. 80, p. 33–44, doi:10.1016/j.lithos.2003.11.001.

David, K., Schiano, P., and Allegre, C.J., 2000, Assessment of the Zr/Hf fractionation in oceanic basalts and continental materials during petrogenetic processes: Earth and Planetary Science Letters, v. 178, p. 285–301, doi:10.1016/S0012-821X(00) 00088–1.

Defant, M.J., and Drummond, M.S., 1990, Derivation of some modern arc magmas by melting of young subducted lithosphere: Nature, v. 347, p. 662–665, doi:10.1038/347662a0.

Defant, M.J., Jackson, T.E., Drummond, M.S., De Boer, J.Z., Bellon, H., Feigenson, M.D., Maury, R.C., and Stewart, R.H., 1992, The geochemistry of young volcanism throughout western Panama and southeastern Costa Rica: An overview: Journal of the Geological Society of London, v. 149, p. 569–579, doi:10.1144/gsjgs.149.4.0569.

Defant, M.J., Xu, J.F., Kepezhinskas, P., Wang, Q., Zhang, Q., and Xiao, L., 2002, Adakites: Some variations on a theme: Acta Petrolei Sinica, v. 18, p. 129–142.

Dewey, J.F., Shackleton, R.M., Chang, C., and Sun, Y., 1988, The tectonic evolution of the Tibetan Plateau: Philosphical Transactions of the Royal Society of London Series A, v. 327, no. 1594, p. 379–413, doi:10.1098/rsta.1988.0135.

Deng, W., 1998, Cenozoic Intraplate Volcanic Rocks in the Northern Qinghai–Xizang (Tibetan) Plateau: Beijing, Geological Publishing House, 180 p.

Deng, W.M., Huang, X., and Zhong, D.L., 1998, Alkali-rich porphyries and relationship related to intraplate metamorphosis in the North part of Jinshajiang zone, Dianxi: Science in China (Series D), v. 28, p. 112–117.

Ding, L., Kapp, P., Zhong, D., and Deng, W., 2003, Cenozoic volcanism in Tibet: Evidence for a transition from oceanic to continental subduction: Journal of Petrology, v. 44, p. 1833–1865, doi:10.1093/petrology/egg061.

Ding, L., Yue, Y., Cai, F., Xu, X., Zhang, Q., and Lai, Q., 2006, ^{40}Ar-^{39}Ar geochronology, geochemical and Sr-Nd-Pb isotopic characteristic of the high-Mg ultrapotassic rocks in Lhasa block of Tibet: Implications in the onset time and depth of NS striking rift system: Acta Geological Sinica, v. 80, p. 1252–1261.

Ding, L., Kapp, P., Yue, Y., and Lai, Q., 2007, Postcollisional calc-alkaline lavas and xenoliths from the southern Qiangtang terrane, central Tibet: Earth and Planetary Science Letters, v. 254, p. 28–38, doi:10.1016/j.epsl.2006.11.019.

Dong, Y.H., 2008, The Post-Collision Magmatism in Doge-Curing-Zhuerken Wula Mountain, North Qiangtang Block, Tibetan Plateau [Ph.D. dissertation]: Beijing, Chinese Academy of Science (in Chinese with an English abstract).

Dong, Y.H., Wang, Q., Xu, J.F., and Zi, F., 2008, Dongyue Lake adakitic volcanic rocks with high Mg# in north Qiangtang block: Petrogenesis and its tectonic implication: Acta Petrolei Sinica, v. 24, p. 291–302.

Fielding, E., Isacks, B., Barazangi, M., and Duncan, C., 1994, How flat is Tibet: Geology, v. 22, p. 163–167, doi:10.1130/0091-7613(1994)022<0163:HFIT>2.3.CO;2.

Galve, A., Jiang, M., Hirn, A., Sapin, M., Laigle, M., De Voogd, B., Gallart, J., and Qian, H., 2006, Explosion seismic P and S velocity and attenuation constraints on the lower crust of the north-central Tibetan Plateau, and comparison with the Tethyan Himalayas: Implications on composition, mineralogy, temperature, and tectonic evolution: Tectonophysics, v. 412, p. 141–157, doi:10.1016/j.tecto.2005.09.010.

Gao, S., Zhang, B.R., Jin, Z.M., Kern, H., Luo, T.C., and Zhao, Z.D., 1998, How mafic is the lower continental crust: Earth and Planetary Science Letters, v. 161, p. 101–117, doi:10.1016/S0012-821X(98)00140-X.

Gao, S., Rudnick, R.L., Yuan, H.L., Liu, X.M., Liu, Y.S., Xu, W.L., Lin, W.L., Ayers, J., Wang, X.C., and Wang, Q.H., 2004, Recycling lower continental crust in the North China craton: Nature, v. 432, p. 892–897, doi:10.1038/nature03162.

Gao, Y.F., Wei, R.H., Hou, Z.Q., Tian, S.H., and Zhao, R.S., 2008, Eocene high-MgO volcanism in southern Tibet: New constraints for mantle source characteristics and deep processes: Lithos, v. 105, no. 1–2, p. 63–72, doi:10.1016/j.lithos.2008.02.008.

Goto, A., and Tatsumi, Y., 1996, Quantitative analysis of rock samples by an X-ray fluorescence spectrometer (II): The Rigaku Journal, v. 13, p. 20–38.

Guo, Z., Wilson, M., Liu, J., and Mao, Q., 2006, Post-collisional, potassic and ultrapotassic magmatism of the northern Tibetan Plateau: Constraints on characteristics of the mantle source, geodynamic setting and uplift mechanisms: Journal of Petrology, v. 47, p. 1177–1220, doi:10.1093/petrology/egl007.

Hacker, B.R., Gnos, E., Ratschbacher, L., Grove, M., McWilliams, M., Sobolev, S.V., Jiang, W., and Wu, Z.H., 2000, Hot and dry deep crustal xenoliths from Tibet: Science, v. 287, p. 2463–2466, doi:10.1126/science.287.5462.2463.

Holbig, E.S., and Grove, T.L., 2008, Mantle melting beneath the Tibetan Plateau: Experimental constraints on the ultrapotassic magmatism: Journal of Geophysical Research, v. 113, B04210, doi:10.1029/2007JB005149.

Hou, Z., Gao, Y., Qu, X., Rui, Z., and Mo, X., 2004, Origin of adakitic intrusives generated during mid-Miocene east–west extension in southern Tibet: Earth and Planetary Science Letters, v. 220, p. 139–155, doi: 10.1016 /S0012-821X(04) 00007-X.

Huang, F., Li, S.G., Dong, F., He, Y.S., and Chen, F.K., 2008, High-Mg adakitic rocks in the Dabie orogen, central China: Implications for foundering mechanism of lower continental crust: Chemical Geology, v. 255, p. 1–13, doi: 10.1016/j.chemgeo.2008. 02.014.

Huang, X.L., Xu, Y.G., Lan, J.B., Yang, Q.J., and Luo, Z.Y., 2009, Neoproterozoic adakitic rocks from Mopanshan in the western Yangtze Craton: Partial melts of a thickened lower crust: Lithos, v. 112, p. 367–381, doi:10.1016/j.lithos.2009.03.028.

Jiang, Y.H., Jiang, S.Y., Ling, H.F., and Dai, B.Z., 2006, Low-degree melting of a metasomatized lithospheric mantle for the origin of Cenozoic Yulong monzogranite-porphyry, east Tibet: Geochemical and Sr-Nd-Pb-Hf isotopic constraints: Earth and Planetary Science Letters, v. 241, no. 3–4, p. 617–633, doi:10.1016/j.epsl.2005 .11.023.

Kadioglu, Y.K., and Dilek, Y., 2010, Structure and geochemistry of the adakitic Horoz granitoid, Bolkar Mountains, south-central Turkey, and its tectonomagmatic evolution: International Geology Review, v. 52, p. 505–535, doi:10.1080/09507110902954847.

Kapp, P., Yin, A., Manning, C.E., Murphy, M., Harrison, T.M., Spurlin, M., Ding, L., Deng, X., and Wu, C., 2000, Blueschist-bearing metamorphic core complexes in the Qiangtang block reveal deep crustal structure of northern Tibet: Geology, v. 28, p. 19–22, doi:10.1130 /0091-7613(2000)28<19:BMCCIT>2.0.CO;2.

Kapp, P., Murphy, M.A., Yin, A., Harrison, T.M., Ding, L., and Guo, J., 2003, Mesozoic and Cenozoic tectonic evolution of the Shiquanhe area of western Tibet: Tectonics, v. 22, p. 1029–1052, doi:10.1029 /2001TC001332.

Karsli, O., Dokuz, A., Uysal, I., Aydin, F., Kandemir, R., and Wijbrans, J., 2010, Generation of the early Cenozoic adakitic volcanism by partial melting of mafic lower crust, eastern Turkey: Implications for crustal thickening to delamination: Lithos, v. 114, p. 109–120, doi:10.1016/j.lithos.2009.08.003.

Kay, R.W., 1978, Aleutian magnesian andesites: melts from subducted Pacific ocean crust. Journal of Volcanology and Geothermal Research, v. 4, p.117–132, doi:10.1016/0377-0273(78)90032-X.

Kay, R.W., and Kay, S.M., 1993, Delamination and delamination magmatism: Tectonophysics, v. 219, p. 177–189, doi:10.1016/0040-1951 (93)90295-U.

Kelemen, P.B., Yogodzinski, G.M., and Scholl, D.W., 2003, Along strike variation in the Aleutian island arc: Genesis of high-Mg# andesite and implications for continental crust, *in* Eiler, J., ed., Inside the Subduction Factory: American Geophysical Union Geophysical Monograph 138, p. 223–276.

Kenzie, D.M., and Priestley, K., 2008, The influence of lithospheric thickness variations on continental evolution: Lithos, v. 102, p. 1–11, doi:10.1016/j.lithos.2007 .05.005.

Klein, E.M., 2003, Geochemistry of the igneous oceanic crust, *in* Rudnick, R.L., Holland, H.D., and Turekian, K.K., eds., Treatise on Geochemistry: Volume 3. The Crust: Oxford, UK, Elsevier-Pergamon, p. 433–463.

Klemperer, S.L., 2006, Crustal flow in Tibet: A review of geophysical evidence for the physical state of Tibetan lithosphere, *in* Searle, M.P, and Law, R.D., eds., Channel Flow, Ductile Extrusion and Exhumation of Lower Mid-Crust in Continental Collision Zones: Geological Society of London Special Publication 268, p. 39–70, doi:10.1144/GSL.SP.2006.268.01.01.

Koppers, A.A.P., 2002, ArArCALC-software for $^{40}Ar/^{39}Ar$ age calculations: Computers & Geosciences, v. 28, p. 605–619, doi:10.1016/S0098-3004 (01)00095–4.

Lai, S.C., and Qin, J.F., 2008, Petrology and geochemistry of the granulite xenoliths from Cenozoic Qiangtang volcanic field: Implication for the nature of the lower crust in the northern Tibetan Plateau and the genesis of Cenozoic volcanic rocks: Acta Petrolei Sinica, v. 24, no. 2, p. 325–336.

Lai, S.C., and Qin, J.F., 2013, Adakitic rocks derived from the partial melting of subducted continental crust: Evidence from the Eocene volcanic rocks in the northern Qiangtang block: Gondwana Research, v. 23, p. 812–824, doi:10.1016/j.gr.2012. 06.003.

Lai, S.C., Liu, C.Y., and Yi, H.S., 2003, Geochemistry and petrogenesis of Cenozoic andesite-dacite associations from the Hoh Xil region, Tibetan Plateau: International Geology Review, v. 45, no. 11, p. 998–1019, doi: 10.2747/0020-6814.45.11.998.

Le Bas, M.J., Le Maitre, R.W., Streckeisen, A., and Zanettin, B., 1986, A chemical classification of volcanic rocks based on the total alkali–silica diagram: Journal of Petrology, v. 27, p. 745–750, doi:10.1093/petrology /27.3.745.

Lee, C.T.A., Cheng, X., and Horodyskyj, U., 2006, The development and refinement of continental arcs by primary basaltic magmatism, garnet pyroxenite accumulation, basaltic recharge and delamination: Insights from the Sierra Nevada, California: Contributions to Mineralogy and Petrology, v. 151, p. 222–242, doi:10.1007/s00410-005–0056–1.

Lee, H.Y., Chung, S.L., Lo, C.H., Ji, J., Lee, T.Y., Qian, Q., and Zhang, Q., 2009, Eocene Neotethyan slab breakoff in southern Tibet inferred from the Linzizong volcanic record: Tectonophysics, v. 477, p. 20–35, doi: 10.1016/j.tecto.2009.02.031.

Lee, H.Y., Chung, S.L., Ji, J.Q., Qian, Q., Gallet, S., Lo, C.H., Lee, T.Y., and Zhang, Q., 2012, Geochemical and Sr-Nd isotopic constraints on the genesis of the Cenozoic Linzizong volcanic successions, southern Tibet: Journal of Asian Earth Sciences, v. 53, p. 96–114, doi: 10.1016 /j.jseaes.2011.08.019.

Li, B.H., Yin, H.S., Lin, J.H., Huang, J.J., and Zhao, B., 2004, A preliminary study of Ar-Ar ages for volcanic rocks from the Mt. Zurhen UI, Qinghai-Tibet Plateau: Acta Geologica Sichuan, v. 24, no. 2, p. 73–76.

Li, C., Cheng, L.R., Hu, K., Yang, Z.R., and Hong, Y.R., 1995, Study on the Paleo-Tethys Suture Zone of Lungmu Co-Shuanghu, Tibet: Beijing, Geological Publishing House, 131 p. (in Chinese with English abstract).

Li, X.H., and McCulloch, M.T., 1998, Geochemical characteristics of Cretaceous mafic dikes from Northern Guangdong, SE China: Age, origin and tectonic significance, *in* Flower, M.F.J., et al., eds., Mantle Dynamics and Plate Interactions in East Asia Geodynamics: American Geophysical Union Geophysical Monograph 27, p. 405–419.

Li, X.H., Liu, D.Y., Sun, M., Li, W.X., Liang, X.R., and Liu, Y., 2004, Precise Sm-Nd and U-Pb isotopic dating of the super-giant Shizhuyuan polymetallic deposit and its host granite, Southeast China: Geological Magazine, v. 141, p. 225–231, doi:10.1017/S0016756803008823.

Li, Y.G., Mo, X., Yi, H.S., Ma, R.Z., Liu, D.Z., and Tao, X.F., 2005, Research on the Cenozoic volcanic rocks in the Cuoli area of Qiangtang: Journal of Mineralogy and Petrology, v. 25, p. 27–34.

Li, Y.L., Wang, C.S., Zhao, X., Yin, A., and Ma, C., 2012, Cenozoic thrust system, basin evolution, and uplift of the Tanggula Range in the Tuotuohe region, central Tibet: Gondwana Research, v. 22, p. 482–492, doi: 10.1016/j.gr.2011.11.017.

Liang, H.Y., Campbell, I., Allen, C., Sun, W.D., Yu, H.X., Xie, Y.W., and Zhang, Y.Q., 2007, The age of the potassic alkaline igneous rocks along the Ailao Shan–Red River shear zone: Implications for the onset age of left-lateral shearing: The Journal of Geology, v. 115, p. 231–242, doi:10.1086/510801.

Lin, J.H., 2003, The Cenozoic High-K Calc-Alkaline Volcanic Rock Series in the Northern Tibetan Plateau: Implications of Crust-Mantle Interaction [Ph.D. dissertation]: Chengdu, China, Chengdu University of Technology (in Chinese with English abstract).

Lin, J.H., Yi, H.S., Zhou, B., Li, B.H., Shi, Z.Q., and Huang, J.J., 2003, ^{40}Ar-^{39}Ar isotopic dating and its implication of Cenozoic volcanic rocks from Zuerkengwula Mountain area, northern Tibetan: Journal of Mineralogy and Petrology, v. 23, no. 3, p. 31–34.

Linnen, R.L., and Keppler, H., 2002, Melt composition control of Zr/Hf fractionation in magmatic processes: Geochimica et Cosmochimica Acta, v. 66, p. 3293–3301, doi:10.1016/S0016-7037(02)00924-9.

Liu, J.F., Chi, X.G., Zhao, X.Y., Zhao, Z., Dong, C.Y., Li, G.R., and Zhao, Y.D., 2009, Chronology, geochemistry and tectonic significances of the Cenozoic Zougouyouchacuo and Nadingcuo volcanic rocks in northern Tibetan Plateau: Acta Petrolei Sinica, v. 25, no. 12, p. 3259–3274.

Liu, S., Hu, R.Z., Feng, C.X., Zou, H.B., Li, C., Chi, X.G., Peng, J.T., Zhong, H., Qi, L., Qi, Y.Q., and Wang, T., 2008, Cenozoic high Sr/Y volcanic rocks in the Qiangtang terrane, northern Tibet: Geochemical and isotopic evidence for the origin of delaminated lower continental melts: Geological Magazine, v. 145, p. 463–474, doi: 10.1017/S0016756808004548.

Lustrino, M., 2005, How the delamination and detachment of lower crust can influence basaltic magmatism: Earth-Science Reviews, v. 72, p. 21–38, doi:10.1016 /j.earscirev.2005.03.004.

Martin, H., 1987, Petrogenesis of Archean trondhjemites, tonalites, and granodiorites from eastern Finland: Major and trace element geochemistry: Journal of Petrology, v. 28, p. 921–953, doi:10.1093/petrology/28.5.921.

Martin, H., 1999, The adakitic magmas: Modern analogues of Archaean granitoids: Lithos, v. 46, p. 411–429, doi.org /10.1016/S0024-4937 (98) 00076–0.

Martin, H., Smithies, R.H., Rapp, R., Moyen, J.F., and Champion, D.C., 2005, An overview of adakite, tonalite–trondhjemite–granodiorite (TTG), and sanukitoid: Relationships and some implications for crustal evolution: Lithos, v. 79, p. 1–24, doi:10.1016/j.lithos .2004.04.048.

Miller, C., Schuster, R., Klotzli, U., Frank, W., and Grasemann, B., 1999, Post-collisional potassic and ultrapotassic magmatism in SW Tibet: Geochemical and Sr-Nd-Pb-O isotopic constraints for mantle source characteristics and petrogenesis: Journal of Petrology, v. 83, p. 5361–5375, doi:10.1093/petroj/40.9.1399.

Mo, X., Hou, Z., Niu, Y., Dong, G., Qu, X., Zhao, Z., and Yang, Z., 2007, Mantle contributions to crustal thickening during continental collision: Evidence from Cenozoic igneous rocks in southern Tibet: Lithos, v. 96, p. 225–242, doi:10.1016/j.lithos.2006.10.005.

Molnar, P.A., 1988, A review of geophysical constraints on the deep structure of the Tibetan Plateau, the Himalaya, and the Karakoram, and their tectonic implication: Philosophical Transactions of the Royal Society of London, ser. A, v. 326, p. 33–88, doi:10.1098/rsta.1988.0080.

Mori, L., Gomez-Tuena, A., Cai, Y., and Goldstein, S.L., 2007, Effects of prolonged flat subduction on the Miocene magmatic record of the central Trans-Mexican volcanic Belt: Chemical Geology, v. 244, p. 452–473, doi:10.1016/j.chemgeo.2007.07.002.

Nelson, K.D., 1992, Are crustal thickness variations in old mountain belts like the Appalachians a consequence of lithospheric delamination: Geology, v. 20, p. 498–502, doi:10.1130/0091-7613(1992)020<0498:ACTVIO>2.3 .CO;2.

Niu, Y., and Batiza, R., 1997, Trace element evidence from seamounts for recycled oceanic crust in the eastern equatorial Pacific mantle: Earth and Planetary Science Letters, v. 148, p. 471–484, doi:10.1016/S0012-821X (97)00048-4.

Owens, T., and Zandt, G., 1997, Implications of crustal property variations for models of Tibetan Plateau evolution: Nature, v. 387, p. 37–43, doi:10.1038/387037a0.

Pan, G.T., Wang, L.Q., Li, R.S., Yuan, S.H., Ji, W.H., Yin, F.G., Zhang, W.P., and Wang, B.D., 2012, Tectonic evolution of the Qinghai-Tibet Plateau: Journal of Asian Earth Sciences, v. 53, p. 3–14, doi:10.1016/j.jseaes .2011.12.018.

Petford, N., and Atherton, M.P., 1996, Na-rich partial melts from newly underplated basaltic crust: The Cordillera Blanca Batholith, Peru: Journal of Petrology, v. 37, p. 1491–1521, doi:10.1093/petrology/37.6.1491.

Pfänder, J.A., Münker, C., Stracke, A., and Mezger, K., 2007, Nb/Ta and Zr/Hf in ocean island basalts: Implications for crust-mantle differentiation and the fate of niobium: Earth and Planetary Science Letters, v. 254, p. 158–172, doi:10.1016/j.epsl.2006. 11.027.

Plank, T., 2005, Constraints from thorium/lanthanum on sediment recycling at subduction zones and the evolution of the continents: Journal of Petrology, v. 46, no. 5, p. 921–944, doi:10.1093/petrology/egi005.

Qiu, H.N., and Jiang, Y.D., 2007, Sphalerite $^{40}Ar/^{39}Ar$ progressive crushing and stepwise heating techniques: Earth and Planetary Science Letters, v. 256, p. 224–232, doi:10.1016/j.epsl.2007.01.028.

Rapp, R.P., and Watson, E.B., 1995, Dehydration melting of metabasalt at 8–32-kbar: Implications for continental growth and crust–mantle recycling: Journal of Petrology, v. 36, p. 891–931, doi:10.1093/petrology /36.4.891.

Rapp, R.P., Shimizu, N., Norman, M.D., and Applegate, G.S., 1999, Reaction between slab-derived melts and peridotite in the mantle wedge: Experimental constraints at 3.8 GPa: Chemical Geology, v. 160, p. 335–356, doi:10.1016/S0009-2541(99)00106-0.

Rapp, R.P., Shimizu, N., and Norman, M.D., 2003, Growth of early continental crust by partial melting of eclogite: Nature, v. 425, p. 605–609, doi:10.1038/nature02031.

Roger, F., Tapponnier, P., Arnaud, N., Schärer, U., Brunel, M., Xu, Z., and Yang, J., 2000, An Eocene magmatic belt across central Tibet: Mantle subduction triggered by the Indian collision: Terra Nova, v. 12, p. 102–108, doi:10.1046/j.1365-3121. 2000.123282.x.

Rohrmann, A., Kapp, P., Carrapa, B., Reiners, P.W., Guynn, J., Ding, L., and Heizler, M., 2012, Thermochronologic evidence for plateau formation in central Tibet by 45 Ma: Geology, v. 40, p. 187–190, doi:10.1130 /G32530.1.

Royden, L.H., Burchfiel, B.C., King, R.W., Wang, E., Chen, Z., Shen, F., and Liu, Y., 1997, Surface deformation and lower crustal flow in eastern Tibet: Science, v. 276, p. 788–790, doi:10.1126/science.276.5313.788.

Royden, L.H., Burchfiel, B.C., and van der Hilst, R.D., 2008, The geological evolution of the Tibetan Plateau: Science, v. 321, p. 1054–1058, doi:10.1126/science .1155371.

Rudnick, R., and Gao, S., 2003, Composition of the continental crust, *in* Rudnick, R.L., Holland, H.D., and Turekian, K.K., eds., Treatise on Geochemistry: Volume 3. The Crust: Oxford, UK, Elsevier-Pergamon, p. 1–64.

Shabanian, E., Acocella, V., Gioncada, A., Ghasemi, H., and Bellier, O., 2012, Structural control on volcanism in intraplate postcollisional settings: Late Cenozoic to Quaternary examples of Iran and eastern Turkey: Tectonics, v. 31, TC3013, doi:10.1029/2011TC003042.

Spurlin, M.S., Yin, A., Horton, B.K., Zhou, J., and Wang, J., 2005, Structural evolution of the Yushu-Nangqian region and its relationship to syncollisional igneous activity, east-central Tibet: Geological Society of America Bulletin, v. 117, p. 1293–1317, doi:10.1130/B25572.1.

Stern, C.R., and Kilian, R., 1996, Role of the subducted slab, mantle wedge and continental crust in the generation of adakites from the Austral volcanic zone: Contributions to Mineralogy and Petrology, v. 123, p. 263–281, doi:10.1007/s004100050155.

Sun, S.S., and McDonough, W.F., 1989, Chemical and isotopic systematics of oceanic basalts: Implications for mantle composition and processes, *in* Saunders, A.D, and Norry, M.J., eds., Magmatism in the Ocean Basins: Geological Society of London Special Publication 42, p. 313–345.

Tan, F.W., Pan, G.T., and Xu, Q., 2000, The uplift of Qinghai-Xizang Plateau and geochemical characteristics of Cenozoic volcanic rocks from the center of Qiangtang: Xizang: Acta Petrologica et Mineralogica, v. 19, no. 2, p. 121–130.

Tapponnier, P., Xu, Z., Rogers, F., Meyer, B., Arnaud, N., Wittlinger, G., and Yang, J., 2001, Oblique stepwise rise and growth of the Tibet Plateau: Science, v. 294, p. 1671–1677, doi:10.1126/science.105978.

Tilmann, F., Ni, J., and INDEPTH III Seismic Team, 2003, Seismic imaging of the downwelling Indian lithosphere beneath central Tibet: Science, v. 300, p. 1424–1427, doi:10.1126/science.1082777.

Topuz, G., Okay, A.I., Altherr, R., Schwarz, W.H., Siebel, W., Zack, T., Satır, M., and Sen, C., 2011, Post-collisional adakite-like magmatism in the Ağvanis Massif and implications for the evolution of the Eocene magmatism in the Eastern Pontides (NE Turkey): Lithos, v. 125, p. 131–150, doi:10.1016/j.lithos.2011.02.003.

Turner, S., Hawkesworth, C., Liu, J.Q., Rogers, N., Kelley, S., and van Calsteren, P., 1993, Timing of Tibetan uplift constrained by analysis of volcanic rocks: Nature, v. 364, p. 50–54, doi:10.1038/364050a0.

Turner, S., Arnaud, N., Liu, J., Rogers, N., Hawkesworth, C., Harris, N., and Kelley, S., 1996, Post-collision, shoshonitic volcanism on the Tibetan Plateau: Implications for convective thinning of the lithosphere and the source of ocean island basalts: Journal of Petrology, v. 37, p. 45–71, doi:10.1093/petrology/37.1.45.

Unsworth, M., Wei, W., Jones, A.G., Li, S., Bedrosian, P., Booker, J., Jin, S., Deng, M., and Tan, H., 2004, Crustal and upper mantle structure of northern Tibet imaged with magnetotelluric data: Journal of Geophysical Research, v. 109, B02403, doi:10.1029 /2002JB002305.

van der Voo, R., Spakman, W., and Bijwaard, H., 1999, Tethyan subducted slabs under India: Earth and Planetary Science Letters, v. 171, p. 7–20, doi.org/10.1016 /S0012-821X(99)00131–4.

Wang, B.D., Chen, J.L., Xu, J.F., Wang, L.Q., Zeng, Q.G., and Dong, Y.H., 2010, Chronology and geochemistry of the Nadingcuo volcanic rocks in the southern Qiangtang region of the Tibetan Plateau: Partial melting of remnant ocean crust along the Bangong-Nujiang suture: Acta Geologica Sinica, v. 84, p. 1461–1473, doi:10.1111/j.1755-6724.2010.00341.x.

Wang, C., Zhao, X., Liu, Z., Lippert, P.C., Graham, S.A., Coe, R.S., Yi, H., Zhu, L., Liu, S., and Li, Y., 2008, Constraints on the early uplift history of the Tibetan Plateau: Proceedings of the National Academy of Sciences of the United States of America, v. 105, p. 4987–4992, doi:10.1073/pnas.0703595105.

Wang, J.H., Yin, A., Harrison, T.M., Grove, M., Zhang, Y.Q., and Xie, G.H., 2001, A tectonic model for Cenozoic igneous activities in the eastern Indo-Asian collision zone: Earth and Planetary Science Letters, v. 188, p. 123–133, doi:10.1016/S0012-821X (01) 00315–6.

Wang, Q., McDermott, F., Xu, J.F., Bellon, H., and Zhu, Y.T., 2005, Cenozoic K-rich adakitic volcanic rocks in the Hohxil area, northern Tibet: Lower-crustal melting in an intracontinental setting: Geology, v. 33, p. 465–468, doi:10.1130/G21522.1.

Wang, Q., Xu, J.F., Jian, P., Bao, Z.W., Zhao, Z.H., Li, C.F., Xiong, X.L., and Ma, J.L., 2006, Petrogenesis of adakitic porphyries in an extensional tectonic setting, Dexing, South China: Implications for the genesis of porphyry copper mineralization: Journal of Petrology, v. 47, p. 119–144, doi:10.1093/petrology/egi070.

Wang, Q., Wyman, D.A., Xu, J.F., Dong, Y.H., Vasconcelos, P.M., Pearson, N., Wan, Y.S., Dong, Y.H., Li, C.F., Yu, Y.S., Zhu, T.X., Feng, X.T., Zhang, Q.Y., Zi, F., and Chu, Z.Y., 2008, Eocene melting of subducting continental crust and early uplifting of central Tibet: Evidence from central-western Qiangtang high-K calc-alkaline andesites, dacites and rhyolites: Earth and Planetary Science Letters, v. 272, p. 2158–2171, doi:10.1016 /j.epsl.2008.04.034.

Wang, Q., Wyman, D.A., Li, Z.X., Sun, W.D., Chung, S.L., Vasconcelos, P.M., Zhang, Q.Y., Dong, Y.H., Yu, Y.S., Pearson, N., Qiu, H.L., Zhu, T.X., and Feng, X.T., 2010, Eocene north-south trending dikes in central Tibet: New constraints on the timing of east-west extension with implications for early plateau uplift: Earth and Planetary Science Letters, v. 298, p. 205–216, doi: 10.1016/j.epsl.2010.07.046.

Wei, G.J., Liang, X.R., Li, X.H., and Liu, Y., 2002, Precise measurement of Sr isotopic composition of liquid and solid base using (LP) MC-ICPMS: Geochimica, v. 31, p. 295–299.

Wei, J.Q., Wang, J.X., and Niu, Z.J., 2004, The Cenozoic volcanic rocks from Chibuzhang Lake area in Qiangtang area: Sedimentary Geology and Tethyan Geology, v. 24, p. 1–21.

Williams, H., Turner, S., Kelley, S., and Harris, N., 2001, Age and composition of dikes in southern Tibet: New constraints on the timing of east-west extension and its relationship to post-collisional volcanism: Geology, v. 29, p. 339–342, doi:10.1130/0091-7613(2001)029<0339: AACODI>2.0.CO;2.

Williams, H., Turner, S., Pearce, J.A., Kelley, S.P., and Harris, N.B.W., 2004, Nature of the source regions for post-collisional, potassic magmatism in southern and northern Tibet from geochemical variations and inverse trace element modelling: Journal of Petrology, v. 45, p. 555–607, doi:10.1093/petrology /egg094.

Wu, F.Y., Huang, B.C., Ye, K., and Fang, A.M., 2008, Collapsed Himalayan-Tibetan orogen and the rising Tibetan Plateau: Acta Petrolei Sinica, v. 24, p. 1–30.

Xia, L.Q., Li, X.M., Ma, Z.P., Xu, X.Y., and Xia, Z.C., 2011, Cenozoic volcanism and tectonic evolution of the Tibetan Plateau: Gondwana Research, v. 19, p. 850–866, doi: 10.1016/j.gr.2010.09.005.

Xiao, L., and Clemens, J.D., 2007, Origin of potassic (C-type) adakite magmas: Experimental and field constraints: Lithos, v. 95, p. 399–414, doi:10.1016/ j.lithos .2006.09.002.

Xiong, X.L., 2006, Trace element evidence for growth of early continental crust by melting of rutile-bearing hydrous eclogite: Geology, v. 34, p. 945–948, doi: 10.1130/G22711A.1.

Xiong, X.L., Adam, J., and Green, T.H., 2005, Rutile stability and rutile/melt HFSE partitioning during partial melting of hydrous basalt: Implications for TTG genesis: Chemical Geology, v. 218, p. 339–359, doi: 10.1016/j.chemgeo.2005.01.014.

Xiong, X.L., Xia, B., Xu, J.F., Niu, H.C., and Xiao, W.S., 2006, Na depletion in modern adakites via melt/rocks reaction within the sub-arc mantle: Chemical Geology, v. 229, p. 273–292, doi:10.1016/j.chemgeo .2005.11.008.

Xu, J.F., Shinjo, R., Defant, M.J., Wang, Q., and Rapp, R.P., 2002a, Origin of Mesozoic adakitic intrusive rocks in the Ningzhen area of east China: Partial melting of delaminated lower continental crust: Geology, v. 30, p. 1111–1114, doi:10.1130/0091-7613(2002)030<1111: OOMAIR>2.0.CO; 2.

Xu, J.F., Castillo, P.R., Li, X.H., Yu, X.Y., Zhang, B.R., and Han, Y.W., 2002b, MORB-type rocks from the Paleo-Tethyan Mian-Lueyang northern ophiolite in the Qinling Mountains, central China: Implications for the source of the low $^{206}Pb/^{204}Pb$ and high $^{143}Nd/^{144}Nd$ mantle component in the Indian Ocean: Earth and Planetary Science Letters, v. 198, p. 323–337, doi:10.1016/S0012 -821X(02)00536–8.

Xu, Q., Ding, L., Zhang, L.Y., Cai, F.L., Lai, Q.Z., Yang, D., and Liu-Zeng, J., 2013, Paleogene high elevations in the Qiangtang terrane, central Tibetan Plateau: Earth and Planetary Science Letters, v. 362, p. 31–42, doi:10.1016/j.epsl.2012.11.058.

Xu, W.L., Wang, Q.H., Wan, D.Y., Guo, J.H., and Pei, F.P., 2006, Mesozoic adakitic rocks from the Xuzhou–Suzhou area, eastern China: Evidence for partial melting of delaminated lower continental crust: Journal of Asian Earth Sciences, v. 27, p. 454–464, doi:10.1016 /j.jseaes.2005.03.010.

Xu, Y.G., Lan, J.B., Yang, Q.J., Huang, X.L., and Qiu, H.N., 2008, Eocene break-off of the Neo-Tethyan slab as inferred from intraplate-type mafic dykes in the Gaoligong orogenic belt, eastern Tibet: Chemical Geology, v. 255, p. 439–453, doi: 10.1016/ j.chemgeo .2008.07.016.

Yin, A., and Harrison, T.M., 2000, Geologic evolution of the Himalayan–Tibetan orogen: Annual Review of Earth and Planetary Sciences, v. 28, p. 211–280, doi:10.1146 /annurev.earth.28.1.211.

Yin, A., Kapp, P.A., Murphy, M.A., Manning, C.E., Harrison, T.M., Grove, M., Ding, L., Deng, X., and Wu, C., 1999, Significant late Neogene east-west extension in northern Tibet: Geology, v. 27, p. 787–790, doi: 10.1130/0091-7613(1999)027<0787: SLNEWE>2.3 .CO;2.

Zhang, H.F., Parrish, R., Zhang, L., Xu, W.C., Yuan, H.L., Gao, S., and Crowley, Q.G., 2007, A-type granite and adakitic magmatism association in Songpan-Garze fold belt, eastern Tibetan Plateau: Implication for lithospheric delamination: Lithos, v. 97, p. 323–335, doi:10.1016/j.lithos.2007.01.002.

Zhang, Z.J., Yuan, X.H., Chen, Y., Tian, X.B., Kind, R.N., Li, X.Q., and Teng, J.W., 2010, Seismic signature of the collision between the east Tibetan escape flow and

the Sichuan Basin: Earth and Planetary Science Letters, v. 292, p. 254–264, doi:10.1016/j.epsl.2010.01.046.

Zhao, Z., Chi, X., Liu, J., Li, G., and Zhao, Y., 2009a, Geochemical feature and its tectonic significance of Gemucuo Oligocene potassic volcanic rocks in the Qiangtang area, Tibet, China: Geological Bulletin of China, v. 28, p. 463–473.

Zhao, Z., Mo, X., Dilek, Y., Niu, Y., Depaolo, D., Robinson, P., Zhu, D., Sun, C., Dong, G., Zhou, S., Luo, Z., and Hou, Z., 2009b, Geochemical and Sr-Nd-Pb-O isotopic compositions of the post-collisional ultrapotassic magmatism in SW Tibet: Petrogenesis and implications for India intra-continental subduction beneath southern Tibet: Lithos, v. 113, p. 190–212, doi:10.1016/j.lithos.2009.02.004.

Zhao, Z.M., Li, R.S., Ji, W.H., Yi, H.S., Lin, J.H., and Zhu, T.X., 2007, The geochemical characteristics and its tectonic significance from the adakite of Paleogene volcanic rocks in northern Qiangtang area, Qinghai-Tibetan Plateau: Journal of China University of Geosciences, v. 32, p. 651–662.

Zheng, X.S., Bian, Q.T., and Zheng, J.K., 1996, On the Cenozoic volcanic rocks in Hohxil district, Qinghai Province: Acta Petrolei Sinica, v. 12, p. 530–545.

Zhou, H.W., and Murphy, M.A., 2005, Tomographic evidence for wholesale underthrusting of India beneath the entire Tibetan Plateau: Journal of Asian Earth Sciences, v. 25, p. 445–457, doi:10.1016/j.jseaes.2004.04.007.

Zhu, D.C., Zhao, Z.D., Niu, Y.L., Dilek, Y., Hou, Z.Q., and Mo, X.X., 2013, The origin and pre-Cenozoic evolution of the Tibetan Plateau: Gondwana Research, v. 23, p. 1429–1454, doi:10.1016/j.gr.2012.02.002.

Science Editor: Christian Koeberl
Associate Editor: Yildirim Dilek

Manuscript Received 26 June 2012
Revised Manuscript Received 14 May 2013
Manuscript Accepted 24 July 2013

Printed in the USA